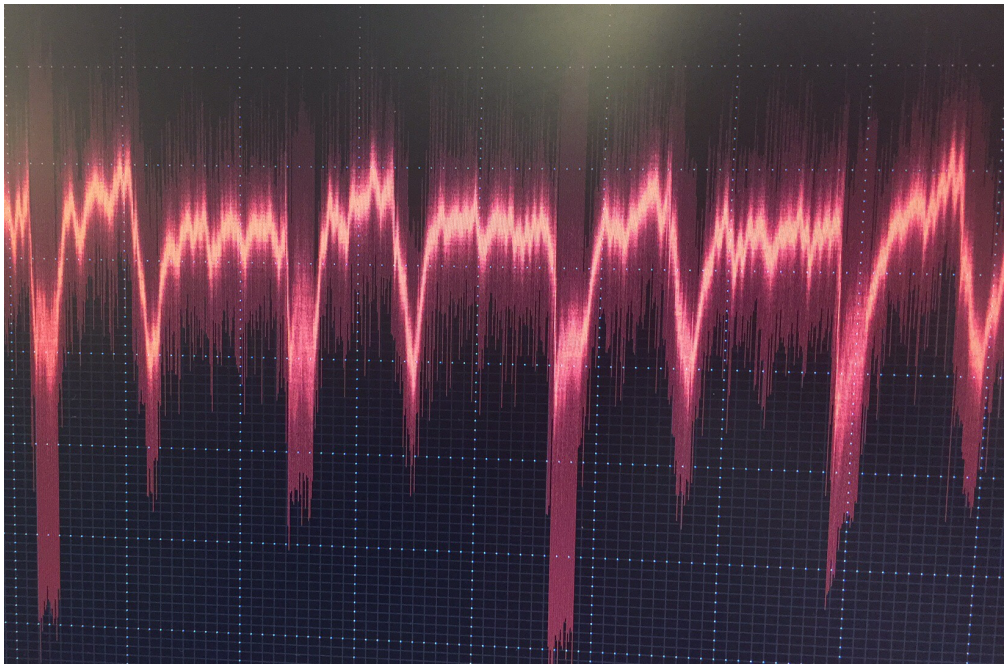

Using High-Speed Sampling for Evaluating Sensor Signals for Fuel Estimation in Common-Rail Injection Systems

MASTER THESIS 2016

AMIR ASKARI, MATHIAS NIEMAND

Department of Computer Science and Engineering
CHALMERS UNIVERSITY OF TECHNOLOGY
UNIVERSITY OF GOTHENBURG
Gothenburg, Sweden 2016

Using High-Speed Sampling for Evaluating Sensor Signals for Fuel Estimation in Common-Rail Injection Systems

A. Askari, M. Niemand

Supervisor: Lena Peterson, Chalmers University of Technology & Agne Holmqvist and Alistair Low, Volvo Group Truck Techology
Examiner: Per Larsson-Edefors, Computer Science and Engineering, Chalmers University of Technology

Master's Thesis 2016
Computer Science and Engineering
Chalmers University of Technology
University of Gothenburg
SE-412 96 Gothenburg
Telephone +46 31 772 1000

Cover: Oscilloscope representation of similar signals investigated in this thesis. The picture show signal decays which is representing pressure decays investigated in this thesis.

Typeset in LaTeX
Gothenburg, Sweden 2016

Using High-Speed Sampling for Evaluating Sensor Signals for Fuel Estimation in Common-Rail Injection Systems

A. Askari, M. Niemand
Department of Computer Science and Engineering
Chalmers University of Technology

Abstract

The minimization of fuel consumption has always been a desirable topic for vehicle manufacturers. There has been research to optimize the engines in several different ways; such as investigating different kinds of fuel, changing engine characteristics and investigations of programmed applications which can be introduced to the engine. There have also been investigations of which different applied injection patterns are most effective for the emissions and engine performance. An engine can operate either with just a main injection or a mixed injection with different setup for pre, main and post injections.

Volvo Group Trucks Technology has decided to investigate possibilities to provide a hardware application in the form of a measuring system for fuel estimation by using signal processing from different sensors in the truck engine. This estimation has to be done in both low and heavy engine-load conditions to be sure that the control is suitable for all operating scenarios for the truck engine.

The scope of this master's thesis is to implement a baseline hardware measuring system using the rail-pressure signal to estimate the injected fuel amount that is compatible with the new microprocessor (method and tool support) that will be implemented to the new product for Volvo. The measuring system is based on using a delta-sigma method for signal processing which is available on the microprocessor. The benefit of using a delta-sigma method for sampling is the noise shifting characteristic which provides the possibility to achieve clear results from the sampling.

In this project, several setups with different levels of fuel injection, high-pressure target in the high-pressure part of the injection system and engine speed have been investigated. To have an outline, the injection pattern was limited to one main injection without pre- or post injection.

To estimate the quantity of injected fuel in each injection, which is equal to the amount of fuel consumed during the injection, a model has been implemented in MATLAB and Simulink to prove the possibilities of this application of the measuring system. This project has also implemented a real-time system for detection of the rail-pressure drop in Eclipse for evaluation of how the delta-sigma ADC on the evaluation board behaved. This proof of concept opens up a basis for further

investigation of real-time system implementation.

Keywords: DSP, High speed ADC (Analog-to-Digital Converter) Micro-Processor, Sensor sampling, Signal sensors, HW (Hardware), ECU (Engine Control Unit)

Acknowledgements

We would first like to express our greatest gratitude to Agne Holmqvist, Alistair Low,
Johan Engbom, Philip Karlsson, Per Pålsson, Igor Lumpus, Bo Person and Shigeki Oobayashi who have helped us throughout this thesis work and made sure that the process of the thesis has turned out as smooth as possible.

Secondly we would like to give our gratitude to Erik Svangård and his group: ECU Installations for providing us with the opportunity to perform this thesis at their department. We have both felt very much as a part of the team and it is not without a bit of sadness that we thank You for this past time.

Finally we would also like to thank Lena Peterson at Chalmers University of Technology who agreed to be our academical supervisor for this thesis. We would like to thank you enormously for helping us with the academic issues that have occurred, report review and the equitable attitude which you have used to push us to perform as high as we possibly could.

Thank You all.

Contents

Abstract

Acknowledgements

Contents **i**

Abbreviation list **iii**

1 Introduction **1**
1.1 Thesis outline . . . 2
1.2 Problem background . . . 3
1.3 Thesis objectives . . . 4
1.4 Method . . . 5
1.5 Limitations . . . 6

2 Technical Background and Theory **8**
2.1 Diesel Engine . . . 9
2.2 Injection System . . . 10
2.3 Injected Fuel-Amount Estimation . . . 12
2.4 Theory and Technical overview . . . 13
2.4.1 Delta-Sigma ADCs . . . 13
2.4.2 Example of Delta-Sigma ADC . . . 17
2.4.3 Processor description . . . 22

3 Experimental Setup in Rig and Software Implementation **26**
3.1 Injection Rig . . . 26
3.1.1 Scenario Set-up . . . 27
3.1.2 Noise reduction in measurement setup . . . 31
3.2 MATLAB and Simulink Evaluations . . . 32
3.2.1 Signal adjustments for processing . . . 32
3.2.2 Simulink model . . . 33
3.2.3 Pressure Drop Detection . . . 34
3.2.4 Temperature Model . . . 34

4 Implementation of Delta-Sigma ADC **36**

4.1 Realtime Implementation of Delta-Sigma ADC 36
4.1.1 Analog Simulations of Rail Pressure 37
4.1.2 TC29x Delta-Sigma ADC 39
4.2 Real-Time Implementation in the Injection Rig 40

5 Results and Discussion **41**
5.1 Result of MATLAB and Simulink 41
5.1.1 Case specific results 43
5.1.2 Temperature investigation results 46
5.2 Results of Delta-Sigma ADC Implementation 47

6 Conclusion **53**

A Appendix **57**

Acronym list

ADC	Analog-to-Digital Converter
AURIX	**A**utomotive **R**ealtime **I**ntegrated ne**X**t Generation Architecture
BM	Bulk Module
CO	Carbon Monoxide
CPU	Central Processing Unit
DS	Delta Sigma
DMA	Direct Memory Access
DSP	Digital Signal Processing
ECU	Electronic Control Unit
EECU	Engine Electronic Control Unit
EMS	Engine Management System
FIR	Finite Impulse Response
GTM	Generic Timer Module
HSSL	High Speed Serial Link
HP	High Pressure
HW	Hardware
LP	Low Pressure
NCV	Nozzle Control Valve
NOX	Nitrogen Oxides
OMV	Outlet Metering Valve
PM	Particulate Matter
SAC	Injector SAC Within the Nozzle
SNR	Signal-to-Noise Ratio
SRI	Shared Resource Interconnect
SW	Software
TC	Tricore

1

Introduction

This project has been executed at Volvo Group Truck Technology (GTT) in the Control Systems Department, ECU-Installation, which is responsible for hardware development of electronic control units (ECUs) for engines.

Volvo GTT covers the entire process from research to final specifications for production of vehicles. Volvo GTT is currently investigating the possibilities for new functions, which can be implemented in their new product line. Within this new product line, the desire is to be on the edge of the newest technology available and to improve performance of the vehicles by having a new ECU implemented.

Effective control of diesel-engine combustion is vital for lowering the levels of pollution, fuel efficiency, noise and vibrations, that are dependent on the whole engine structure. It is therefore difficult to determine effectiveness of combustion due to the large amount of different contributing factors. Because of this it is of great importance to have an accurate fuel-injection control. An engine is constantly operating at changing speed and load in different ambient conditions affecting the exhausts composition, fuel efficiency, noise and vibrations.

There are requirements and regulations on vehicles that are constantly being updated and therefore it is necessary to implement a smart technology to meet these requirements. Two of these regulations are engine emissions and fuel consumption. To fulfill the requirements, there has to be a more precise parameter control by the ECU. The currently new developed ECU is believed to improve performance, and together with a measuring system possibly provide the desired level of control.

By access to a measuring system providing accurate control of the fuel consumption and engine emissions, Volvo will have a better control of the vehicle and the engine performance. As a result, it would be possible for Volvo to provide a better assistance for their customers with respect to diagnostics and maintenance of the vehicles.

1.1 Thesis outline

The main purpose of this thesis project is to implement a measuring system by using rail-pressure evaluation to control the amount of injected fuel. The rail-pressure data is obtained from a sensor located in the common-rail in the injection system of the engine. The measuring system may be implemented in the new ECU that will be available for the new product line.

The reason for having the new type of ECU is to achieve a better performance than for previous generations. The thesis scope is to investigate how the data can be processed and evaluate if it is possible to extract more significant results than previously possible. One of the improvements in the ECU is the access to the higher sampling rates in the delta-sigma analog-to-digital converter (delta-sigma ADC). The signals obtained from an injection system are noisy and contain a lot of pressure variations due the physical properties of the fuel injections and the pumping within the system. Because of these properties of the injection system, it is believed that by using the higher sampling rate and a delta-sigma ADC, it will be possible to obtain more significant data from the injection system for estimation of the amount of fuel injected.

The data gathered in the test rig will give an offline implementation and evaluation of a software model of our measuring system. Software model investigations and verifications of the performance of the delta-sigma ADC can be made before integrating it onto the ECU.

By using this method, it will be possible to estimate the fuel amount through the knowledge of rail-pressure variation. The results of this research may lead to new data evaluations that can be used for higher accuracy in optimization of engines.

1.2 Problem background

New engine demands such as fuel efficiency and less pollution from engines in the EURO-regulation are becoming more strict (see table 1.1). Volvo is therefore forced to develop new ways to keep up with the demands. In the previous ECU, the possibilities of sampling with the available ADCs were restricted. The data from engines are gathered in a noisy environment and have a noisy characteristics. As a result, the processing of these data has been difficult. Because of the availability of the higher sampling rate in the new ECU, Volvo has decided to investigate what can be achieved with this kind of implementation on the new ECU. The first part of this investigation has been assigned to this thesis project. The thesis project has investigated the fundamental implementation for the new possibilities of higher sampling speed to process the sensor data and if it can be used for accurate estimate amount of injected fuel.

Table 1.1: The table below show the European Emission Regulation Standards [8]. Starting at year 1992 until today there have been several legislation for emissions from heavy-duty vehicles as presented below. The emissions presented are: nitrogen oxides (NOX), particulate matter (PM) and carbon monoxide (CO).

	Year	NOX mg/kWh	PM mg/kWh	CO mg/kWh
Euro I	1992	8000	612	4.5
Euro II	1998	7000	150	4.0
Euro III	2000	5000	100	2.1
Euro IV	2005	3500	20	1.5
Euro V	2008	2000	20	1.5
Euro VI	2013	400	10	1.5

The problem addressed by this thesis is the investigation of possibilities for implementing a new method of estimating the injection timing and fuel quantity by processing the rail-pressure sensor information. There have been previous investigations at other companies using the rail pressure to determine fuel amount. However, the results of these investigations are not published in the public domain. In contrast to our work, these investigations were neither done using particularly high-speed sampling nor by using delta-sigma ADC. Because of the low sampling rate, the previous studies showed that there were difficulties in estimating small amount of fuel that are used as pre- and post injections. The higher sampling rate and the properties of noise shaping, which are well-known and will be explained in section 2.4.1 for delta-sigma ADC, are believed to reduce these difficulties of processing the data and give better results.

1.3 Thesis objectives

As previously mentioned the purpose of the project was to investigate measurements of rail pressure, processed by using delta-sigma ADC. Previously, the delta-sigma ADC has not been available and due to the low sampling rate available in the ECU, the successive-approximation ADCs have been used with the low sampling rate for evaluation of sensor signals. The main objectives for this thesis have been:

- Implementation of delta-sigma ADC setup for achieving the rail-pressure data evaluations in software
- Estimating the fuel temperature in order to estimate the fuel consumption
- Establishing a measurement system for the injected amount of fuel and injection timing by using rail pressure by:

  - Investigating how the measured data provides information of the amount of injected fuel

  - Investigating how the measured data provides information about injection timing (when the fuel injector is open/closed)

The first objective within this thesis project is to gather significantly valid data from the injection test rig. Significant and correct data are determining factors in evaluations and analysis. The rail pressure is the most important data to obtain, but also the nozzle control valve (NCV) signal and injection-sac (SAC) pressure are important. Both the NCV signal and SAC pressure provide more accurate information about the injection timing than possible by only using the rail pressure, and information about injection duration. Due to the relation between the fuel injection timing and injection duration in the engine, there cannot be any proper evaluation by just knowing the pressure variance. It is also necessary to know the correlation with other additional signals.

The second objective is to establish the measuring system and implement it into software. Configuring the Simulink model of the delta-sigma ADC provided from the manufacturer Infineon [2] is the main part of this task. It is also necessary to locate the pressure drop in time during the injection and not to include disturbance oscillations into the pressure drop deterministic. The pressure drop should therefore only be estimated during the time when the SAC pressure is active.

The third objective is to estimate the injected fuel amount by implementation of the model in software. Once the pressure drop during the injection is determined, it is possible to calculate and estimate the amount of injected fuel, since the pressure drop is proportional to the amount of injected fuel.

The final objective is to configure the delta-sigma ADC on the Infineon AURIX starter kit TC29x [17]. By setting up the model similar to the Simulink model, the measurement system can be implemented in hardware. An issue with implementing the measurement system in hardware is that an actual engine does not have the additional data information such as SAC nor the actual injected amount of each injector that can be observed and measured from the injection test rig. However, in Volvo's ECU, there are models instead of sensors determining some of the necessary parameters. These models are set up for a particular engine type and they depend of the entire engine structure. This is not the case for the test rig since the combustion is not included. The influence of the combustion is therefore not included in the test rig measurements. Other parameters, such as bulks modulus (elastic properties of the fuel), that can not be obtained by models in the engine have to be hardware implemented. This will have some effects of uncertainty for estimating the injected fuel amount

1.4 Method

The project work plan was divided into the presented main objectives. To be able to achieve the first objective, a fundamental understanding of the injection system is necessary. There are several different kinds of fuel injection systems and this thesis project has only focused on the common-rail injection system. In common-rail injection system, there are some physical phenomena, e.g wave propagation within the rail, which have to be taken into consideration when determining the pressure drop. The knowledge of the common-rail injection system has been obtained through a literature study, which will be referred to in section 2.2.

The scenarios performed in the injection test rig were established by Volvo engineers to reflect different true circumstances in which the engine usually operates. The operating parameters that varied between the scenarios were: revolutions per minute (rpm), injected fuel amount and target pressure within the rail. Since one of the accomplishments of this project is the evaluation of the amount of fuel, several more variations of injected fuel amount were targeted in the measurements than for the other parameters: rpm and target pressure.

After each scenario the gathered data was saved, the settings of the next scenario was set and the data was then stored in the same procedure as previous scenario. To limit disturbances in the measurements, the break-out box connected to the injection rig is bypassed and the rail-pressure signal is obtained directly from the sensor. The data was gathered by using a Yokogawa oscilloscope[18] where the sampling frequency is chosen for an appropriate window size.

The Yokogawa oscilloscope stores the waveforms for each measurement scenario. After that, to be able to handle the waveform data, it is necessary to export these data of scenarios from Yokogawa software (Xviewer), which could later be imported through a Volvo in-house MATLAB function into MATLAB. Once the measurement data have been imported, the data processing and implementation of the software measuring system can be done through MATLAB coding and the delta-sigma ADC Simulink model to evaluate both the pressure drop and the fuel amount.

The measuring system has been modelled in software through MATLAB and Simulink. The implementation of the evaluation board from Infineon, on which the microprocessor is integrated, is set up through the free Tricore tool chain [19] based on the Eclipse environment. In the Eclipse environment, the delta-sigma ADC needs to be configured. Since within this stage of the thesis, the additional parameters like rail temperature and SAC-pressure or NCV are no longer available, they have to be analyzed through the software implementation. For a desk implementation of the evaluation board, the rail-pressure signal had to be simulated using function generators.

1.5 Limitations

Within the thesis project there are limitations that will not be discussed in detail. One of the limitations in the project is that the investigation will only focus on the rail-pressure sensor in the fuel-injection system as desirable evaluation data. The main reason for investigating the rail pressure is that data can be obtained quickly from the test rig and measured during other ongoing tests. In this way it does not delay the thesis work nor interfere with Volvo's own activities in the test rig.

The measurement data of rail pressure is also limited to one single injection pulse. Usually the injection made is accompanied by both pre- and post-injections. The injection is varied throughout the measurement scenarios from normal main-injections down to the quantities that are used for pre-injections (pilots) and post-injections. This limitation is applied to reduce the complexity of the input data and to improve the interpretation of the results. Although this is not a fully efficient scenario for the engine and is most often avoided, since injections are more often made in smaller time periods with varied fuel amounts. This implementation of the injection will provide an outline to what injection levels can be seen in the results, since all injections have common pressure-variation properties of the common rail. The properties of the common rail are also properties of the whole injection system.

Another limitation in the project is that the data were collected in a high-pressure fuel injection rig (an engine without a combustion system). The gathered data and other settings in the injection rig have been specified for different cases. The construction of the injection rig may therefore contribute with some errors that may not occur similarly in an actual engine. Errors other than temperature estimation

are not included in this thesis.

Since the measurement measures pressurized fluid within a cavity, there are theoretical calculations for estimating the pressure variations. The theoretical principle for estimating the calculations will not be taken into any larger consideration, since this is not the main objective of the project. The collected data will also only be used for evaluations of the quantity of injected fuel. The implementation will therefore not be used as feedback-control to control the injected fuel amount and eliminate possible error in the injected fuel amount. By this the project will only discuss the injected fuel as an estimation or evaluation of the collected data, and the focus will be on the results of the rail pressure that have been obtained.

The investigation of this thesis was only made on the AURIX Tricore microprocessor. This microprocessor will be a part of the new ECU at Volvo and is the latest generation powertrain microprocessors available. There is therefore no interest in investigating different types. This will also, by default, lead to the limitation of Infineon providing Simulink and software-framework models for the microprocessor as well as implementation code examples.

2

Technical Background and Theory

The common-rail injection system is the one of the fuel-injection systems applied in Volvo diesel engines. The common-rail application to an injection system is a well known concept throughout the continuously development of diesel engines from the early 20^{th} century and still is being further developed today [10].

Unlike other types of injection systems, the common-rail injection system supplies a high pressured fuel independent of the engine speed [10]. The pressure is obtained and kept in the rail enclosure. This offers the opportunity to tune the rail pressure target within the rail enclosure to provide lower emissions and achieve higher rotational force (torque).

The higher engine torque enables the engine to handle larger loads. More load on the engine normally requires more injected fuel. This provides a rich fuel mix (high fuel to air ratio) and a cold combustion will take place. Cold combustion is not always the preferable case due to the inefficient fuel usage, wear of the engine and higher emissions of carbon dioxide (CO_2). By injecting less fuel, the fuel mix will not be as rich and a so-called warm combustion will take place and result in a different emissions mix than for the cold combustion with a higher amount of nitrogen oxides (NOx). To optimize this trade-off of emissions and fuel usage it is therefore desirable to use the specific amount of fuel at the specific engine speeds and loads. The common-rail injection system supplies the possibilities to modulate the injection pattern and therefore optimize the balance between cold and warm combustion [12].

2.1 Diesel Engine

The first diesel engine was introduced by Rudolf Diesel in the 1890s. The first-generation diesel engine was large with a low operating speed [4]. The new kind of engine was noticeably more efficient than the steam engines that were commonly used for industries. At first, Rudolf Diesel wanted to use coal, but later decided to use liquid oil instead. Nowadays, all diesel engines use some kind of diesel oil mixture (fossil, synthetic, bio).

After some time, diesel engines were installed in vehicles. One of the first diesel engines for a vehicle was introduced in the early 1920s by Benz, used in a three-wheeled tractor [4].

The first diesel engine by Volvo was introduced in 1946 (planned to be introduced in 1940, but was delayed because of World War II). This engine was called VDA (Volvo Diesel engine type A) and the vehicle in which this engine was included became one of the most famous trucks in Sweden [7].

Diesel engines have the beneficial characteristics of consuming less fuel, being more durable and more reliable than petrol engines. However, an issue with diesel is that the combustion process results in emissions of NOx, CO_2 and particulate matter (PM) [3], which are also the subjects of regulations presented in table 1.1.

The two main factors that contribute to diesel combustion process are:

- Inducted amount of air in the cylinders (temperature and kinetic energy dependent)
- Injected fuel (temperature, injection duration, common-rail-target pressure and physical characteristics dependent)

The amounts of NOx and CO_2 emissions depend upon the type of combustion. When the engine executes a cold combustion with rich fuel-air mix, the engine emits a higher amount of CO_2 (which is a result of complete combustion of carbon monoxide CO). When the fuel mix has a high quantity of air, a warm combustion occurs and the amount of NOx emission is higher. To achieve the low levels of NOx and CO_2 specified in legislation (see table 1.1), the combustion must be optimized, so that neither the amount of CO_2 nor NOx emitted is too high. It can also be seen in table 1.1 that the regulations for pollution have become stricter throughout the years.

Through the benefits of the common-rail injection system, the injected fuel as main factor for diesel combustion can be optimized. By investigating how well the injected fuel can be observed and controlled for the common-rail injection system, further optimizations can be made and provide new possibilities for decreasing the emissions.

2.2 Injection System

The injection system of a diesel engine consists of four parts: the high-pressure (HP) system, low-pressure (LP) system, ECU and the after-treatment hydrocarbon injector (AHI), as can be seen in figure 2.1. The project of this thesis has limited the injection system into two parts: the HP system and the software components (ECU SW/HW).

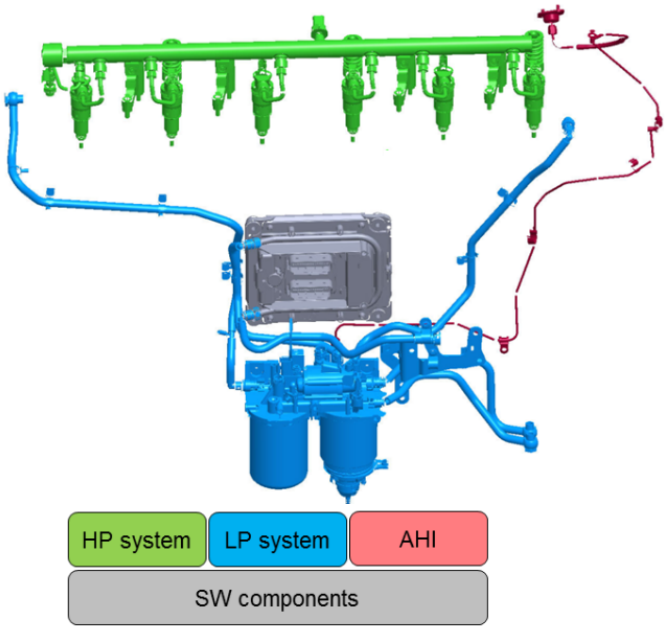

Figure 2.1: Above is an overview of the whole injection system within an engine. The injection system is shown with four subsystems even though only the HP system and SW components have been investigated in this thesis project. (Image used with permission by Volvo GTT)

The common-rail injection system is a HP system and consists of a HP fuel pump, a rail enclosure called common rail, and injectors. The common rail and injectors can be seen in figure 2.2. The ECU controls the HP system and injectors by assigning a target pressure in the rail that is supplied from the HP fuel pump and controlling the injection timing and duration.

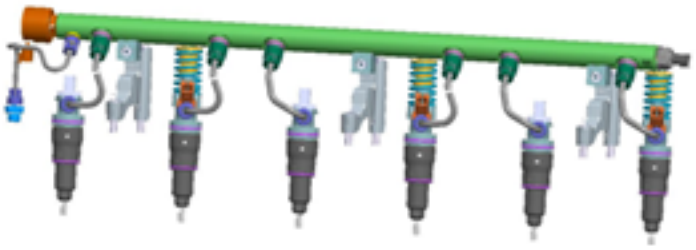

Figure 2.2: A representation of the common rail within the HP system of the injection system. As can be seen the common rail is just a rail where the injectors are connected which are represented. The image shows two types of injectors, to the very left is a injector that only injects fuel and to the right is a injector which can also pump back the fuel. The pumping of the injectors was both varied and turned off during the measurements. (Image used with permission by Volvo GTT)

Since the ECU controls the injection and the HP-fuel pump, the implementation on the ECU contributes to the important functions such as fuel delivery, injection time, injection-rate modulation and through these functions also controls the combustion.

In the rail, there is a pressure sensor installed to monitor the common-rail pressure. The reason for having this sensor is to detect if the pressure becomes too high for the rail to contain the pressure or if the rail cannot hold the target pressure constant due to leakage.

The common-rail pressure is set to a target value that depends on the engine operating conditions. The HP fuel delivery to the rail is controlled, by the ECU, from the HP fuel pump through the outlet metering valve (OMV). When the injectors inject high-pressured fuel through the injection-needle (NCV) the rail pressure will drop since the fuel is released from the rail into the combustion chamber. This pressure drop can be monitored through the signal from the pressure sensor. This relation between the fuel injection and the rail-pressure drop is the main subject of this project for estimating the injected fuel amount.

An important aspect of the common rail is that wave dynamics can occur due to injections and pumping. These phenomena will show up as oscillations in the measurements. It is important to be aware of these oscillations. Because of these oscillations the most difficult challenges are to distinguish the disturbance oscillations from wave propagation and data oscillations due to the injection. The oscillations can have very high amplitude in the case of standing waves in the rail and are usually located in the low-frequency domain. They might anyway give errors in the determination of the pressure drop if the max or min estimations are located in a wave oscillation minimum or maximum. This uncertainty will then be included in the estimation of the injected fuel amount.

2.3 Injected Fuel-Amount Estimation

As mentioned previously, the injected amount of fuel is proportional to the pressure decay within the common rail during an injection. There are two factors that are of significance for the fuel estimation: the properties of the injection system, and the properties of the fuel. To estimate the injected fuel amount it is possible to use the definition of bulk modulus defined in [16], with the physical definition of the derivative of density over time ($\frac{d\rho}{dt}$) equal to the mass quantity over volume, bulk modulus can be expressed as:

$$B = \frac{dp}{d\rho}\rho \rightarrow \frac{dp}{dt} = \frac{B}{\rho}\frac{d\rho}{dt} \rightarrow \Delta P = \frac{B}{\rho}\frac{Q}{V} \tag{2.1}$$

where $\frac{dp}{dt}$ is the pressure drop ΔP.

From the derivation in (2.1), the estimation of the injected fuel amount, Q, can be expressed as:

$$Q = \frac{\Delta P\ V}{B}\ \rho \tag{2.2}$$

where ΔP is the pressure drop within the common rail during an injection, V is the dead volume which is the fuel volume of the HP injection system (estimated as a constant) and ρ is the density of the fuel.

The pressure drop during the injection and the dead volume signify the properties of the injection system. As mentioned, the pressure within the common rail will decrease during an injection and increase when fuel is pumped into the rail. An outcome of this, the decay of the pressure will originate from the target-rail pressure and down to a value that corresponds to the quantity that has been injected. To obtain the target-rail pressure, fuel is pumped by the HP fuel pump and the common-rail pressure is increased again.

The other parameter of the injection system is the dead volume. The dead volume is a constant within the HP injection system. Given the dependency of dead volume the injected fuel amount will be relative to the amount of fuel which is available within the system.

The other two entities, ρ and B in (2.2), are both properties of the fuel. One of these contributing parameters is the density of the fuel. In this project the density has been approximated to be constant. This is because if the density changes in the fuel it will influence the whole injection system causing a huge effect on the combustion. Since the density is defined as mass over volume a change in density would either result in a change in volume or mass. As mentioned it is known that the volume (dead volume) is constant. This results in that a change in density would result in a change in mass. A change of mass may occur, but is neglected because of the high fuel pressure of the measurements. Thus density is therefore also assumed to be constant.

The last parameter which has to be obtained for the fuel estimation is the bulk modulus. This parameter defines how the elastic properties of fuel vary during temperature and pressure changes. The dependency for how bulk modulus changes in fluids is described in (2.3), which is obtained from ISO 4113 [13]:

$$B = (0.9(17579 - 90\ T) + (4.89 + 0.0052\ T)\ P\ 10^{-5})10^{-5} \tag{2.3}$$

where T is the fuel temperature in degrees Celsius and P is the target-rail pressure expressed in Pascal. A higher value of bulk modulus means a lower compressibility of the fuel.

There have been a lot of research on the thermophysical properties of fluids such as diesel fuel [14]. Chorazewski and collaborators[14] have investigated result of air solubility in the fuel by using ISO 4113 [13] with the temperature span from $0-150$ degrees Celsius and pressure span up to 200 MPa to determine the isothermal bulk modulus of the fuel. The research shows that bulk modulus increases linearly with pressure at low temperatures, but at high temperatures and high pressures a tendency of peak level is shown [14]. It has also been shown that bulk modulus decreases due to a temperature increase. This can also be seen in (2.3). Since the bulk modulus is strongly dependent on the temperature, the fuel quantity estimation will also be highly temperature dependent.

2.4 Theory and Technical overview

In this project, there are functions that must be mentioned to be able to follow the content the project. The delta-sigma ADC converter is the main function of this project and will be presented below. Furthermore, filtering and microprocessor details will be explained.

2.4.1 Delta-Sigma ADCs

The delta-sigma ADC is an ADC which has been developed with specific characteristics [1]. These characteristics are obtained from digital system techniques. The purpose of having an ADC is to convert from an analog input to a digital output. This is done by sampling the signal and then quantizing the samples into bit levels (discrete values). The quantization process assigns a representation from the samples that are still in the analog domain to the digital domain as a binary number. In delta-sigma ADC, approximately one quarter of the conversion is in analog domain and three-quarters are digital domain[1].

Each assigned binary number is represented as a voltage level. The number of voltage levels is described as 2^L, where L is the number of bits, e.g 4 bits would result in 16 voltage levels. The number of voltage levels is exponentially increasing with the number of bits. If the input has a high dynamic range of data, the digital representation will have to consist of an even larger amount of voltage levels, e.g if the amount of data is instead 32 bits then the separate voltage levels will be $42,94,967.296$. The quantization will result in an error included in the sampled signal as shown in figure 2.3. The quantization error does however decrease when using a higher sampling rate (oversampling) due to that the noise-power spectrum will be distributed across a wider frequency range. Using an ADC the signal-to-noise ratio (SNR) should preferably be as high as possible in order to obtain a good representation in the digital domain since the amplitude of the signal is low. The SNR can be described according to (2.4). Since the input is perceived to be constant the only way to improve SNR is to lower the quantization noise[6].

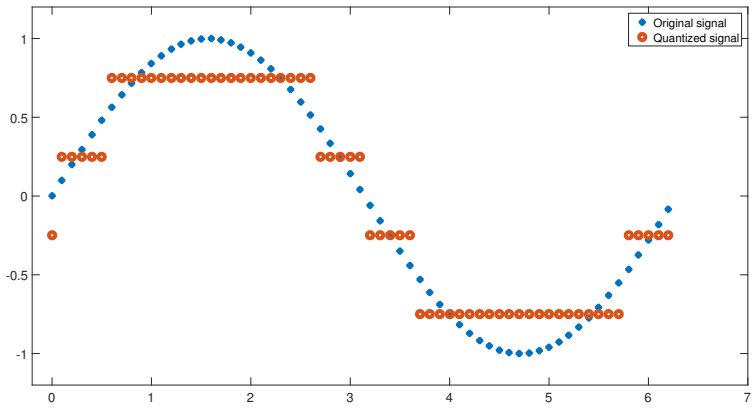

Figure 2.3: This figure shows a representation of a sinusoid input signal together with four quantization levels. As can be seen the sinusoid input will be distorted and noise will occur in the border-line of the peak and valley.

The relation between the signal power and total noise in the system is called SNR. The SNR and input signal are proportional in terms of power:

$$SNR = \frac{\frac{1}{N}\int_t s(t)^2}{\frac{1}{N}\int_t y(t)^2} = \frac{\int_t s(t)^2}{\int_t y(t)^2} \tag{2.4}$$

where $s(t)$ is the power of the input and $y(t)$ is the quantization-noise power. It means that if the input power increases, the SNR will be increased. Theoretically, maximum SNR can be seen at the highest allowable spectral-input power to the system, but in practice, it might be affected by distortion or other reasons.

Signal processing tasks in the digital area are expanding and the need of digital signal processing (DSP) is increased. However, technology is getting continuously more complex and data remain analog[5]. Therefore, the data need to be encoded into the digital domain. To convert analog to digital is important for computational part of the circuits. Accuracy and speed are critical for this conversion. Usually,

analog input enters the converter after being filtered and amplified. The input is then converted to digital data, by a carrier onward to the DSP part. An analog input can mainly be converted to digital data by using two methods: Nyquist rate sampling and oversampling. In Nyquist-rate method, matching can cause accuracy and linearity problems in the converter, and in many DSPs, linearity and accuracy are main part of the requirements.

In an oversampling method, the sampler samples at a much higher rate than the Nyquist rate but with lower resolution than is required by the SNR requirements. These two changes can fix the linearity and accuracy problems. Increasing the sampling frequency improves the SNR by spreading the noise over a larger frequency band. Formula (2.5) shows the SNR for a full-range-sinusoidal wave where N is the number of output bits and oversampling (OSR)[11]:

$$SNR = 6.02 \times N + 1.76 + OSR \tag{2.5}$$

Formula (2.6) shows how oversampling can improve the SNR by applying an oversampling factor K:

$$OSR = 10 \times log \quad (K) \tag{2.6}$$

As an outcome of (2.5) and (2.6), SNR can be improved by 3 dB with oversampling factor of 2. This is a highly important fact to the delta-sigma ADC for determining the required oversampling-rate for obtaining the necessary SNR [15]. To obtain the correct representation of the signal it has to be decimated with the oversampling factor.

Moreover, noise shaping loop shifts the quantization noise to the higher frequencies, which can be filtered out by low-pass filter [1]. There exist different architectures for this method. Mainly, the loop order is different, a higher loop order can improve the SNR at a cost of potential stability issues. The simplest delta-Sigma ADC has first-order delta sigma noise shaping loop. Figure 2.4 shows the first-order loop architecture.

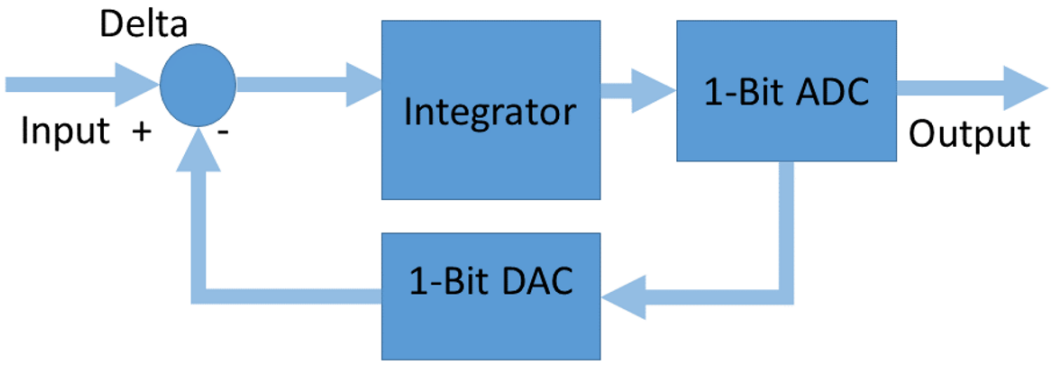

Figure 2.4: This figure shows first-order architecture of ADC consists of integrator together with 1-bit ADC; moreover, DAC is converting digital signal to analog as a feedback part of the delta-sigma ADC. Since 1-bit ADC convert signals into 1-bit, conversion is linear and there is no need to be worried about non-linearity.

The higher-loop order increases the complexity and therefore also increases the potential of introducing instability. Figure 2.5 illustrates the second-order delta-sigma loop. As shown in the picture, it is more complex than the first order.

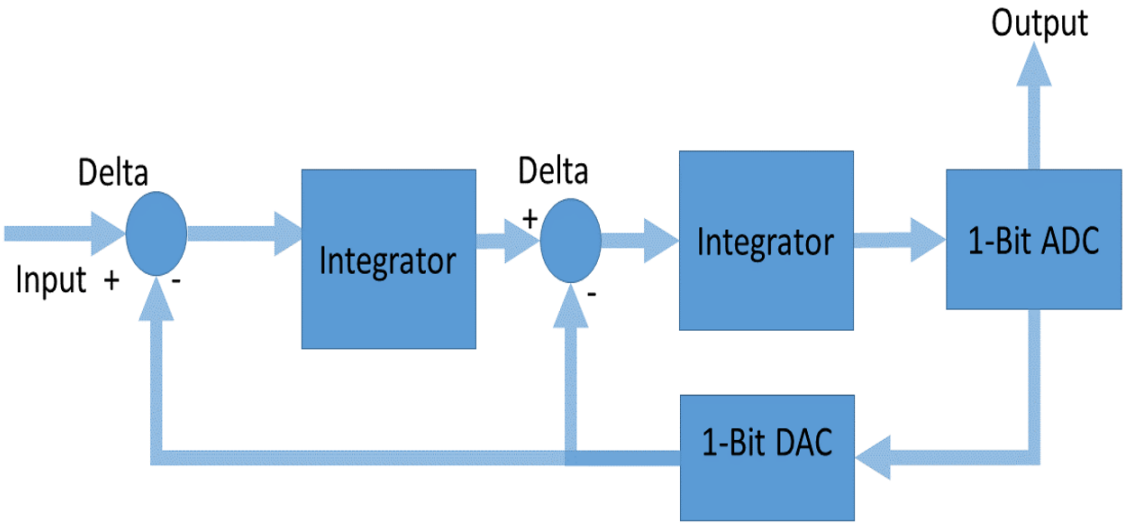

Figure 2.5: This figure shows a general architecture of second-order delta-sigma ADC. It shows that first-order ADC cascade with another first-order ADC to reduce noise. The reason of using the first-order delta-sigma ADC is to keep the system linear.

As mentioned previously, higher loop order increases complexity and potential instability. An alternative way to increase the SNR without adding complexity and instability is cascading two lower-order delta-sigma ADCs. This structure is called **M**ulti-St**A**ge Noise **SH**aping (MASH) delta-sigma ADCs [9]. Figure 2.6 shows the MASH structure. An example of a MASH is if both stages have a second-order delta sigma loop in their modulator, the noise shaping behaves as a fourth-order single loop with a second order instability behavior. As a result, while having a less complicated module, higher SNR can still be achieved. As shown in figure 2.6, two different filters can adjust the signal separately.

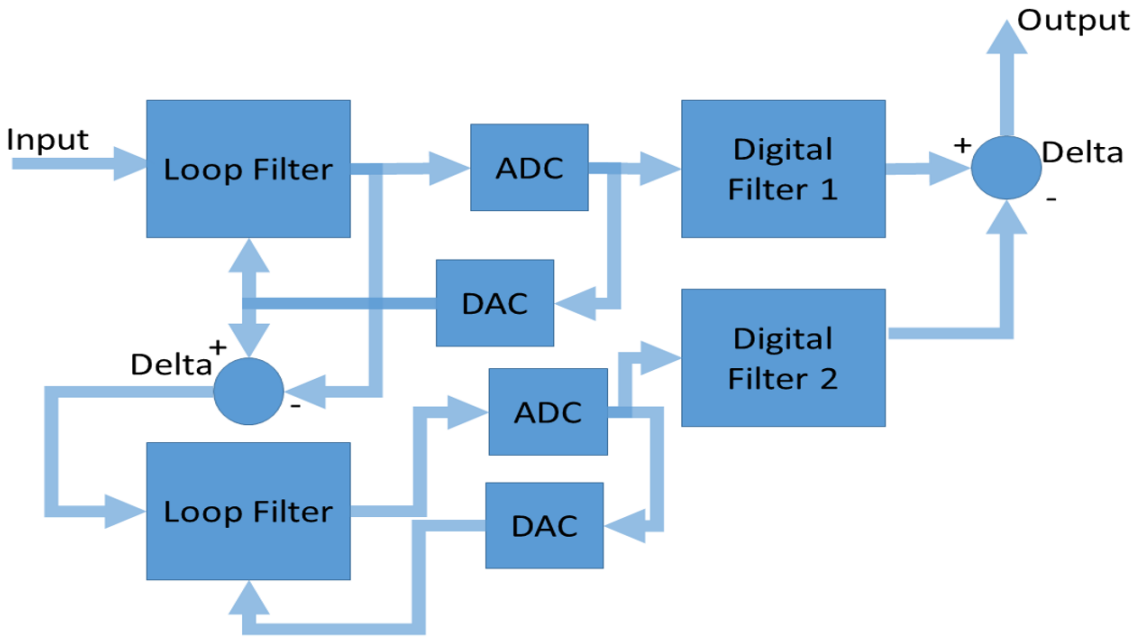

Figure 2.6: This figure shows a multi-stage delta-sigma modulator (MASH) with 2 stages. The MASH model can be increased with a preferable number of stages. This does however make the modulator more complex which is not always preferable.

2.4.2 Example of Delta-Sigma ADC

The processing of the delta-sigma ADC from analog input to digital output can be seen in figures 2.7-2.13. Figure 2.7 shows a sinusoid that in this example represents the input signal. The delta-sigma ADC first processes the input by an oversampling modulator that over-samples the signal. Through a pulse-width modulator (PWM) the signal is converted into a pulse-width-modulated signal that is oversampled, shown in figure 2.8. Within the oversampling the signal has both been sampled and quantized.

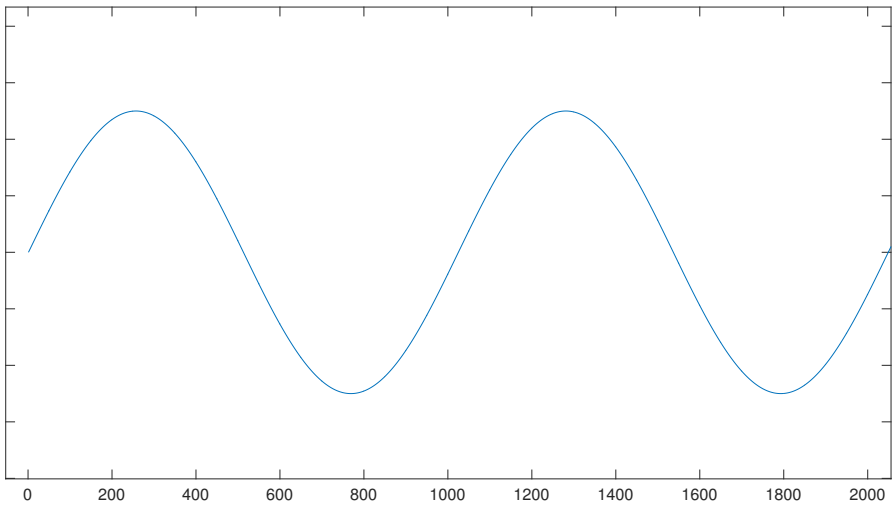

Figure 2.7: This figure shows a representation of a sinusoid wave which can be used as an input to the delta-sigma ADC (shown in figure 2.16). The sinusoidal wave is a very basic example input that can be obtained from any signal generator.

The delta-sigma modulator modulates the analog input to digital value in the delta-sigma ADC. It converts the analog input to a PWM signal. Figure 2.8 shows the time-domain conversion. The figure shows a high speed, one bit pulse width modulated signal.

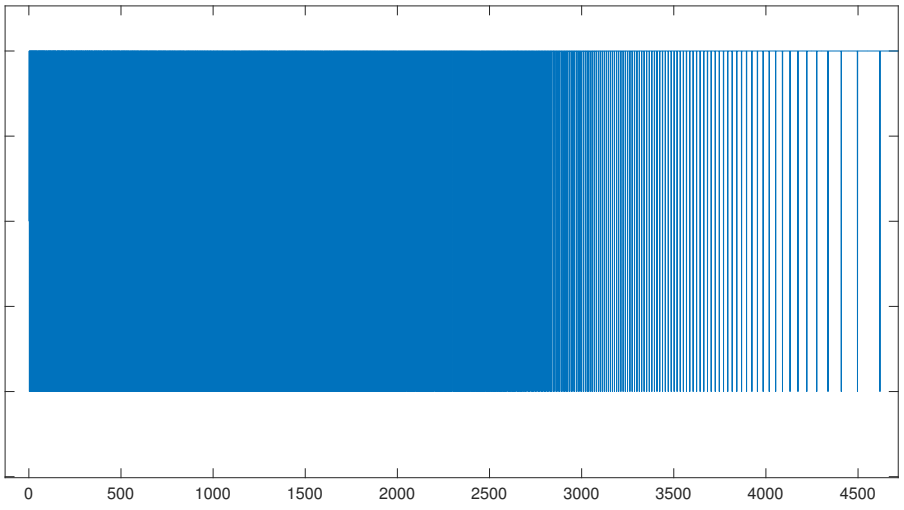

Figure 2.8: This figure shows a representation of delta-sigma pulse width modulated signal. The representation shows the first process stage at the analog delta-sigma modulator block in figure 2.16. As shown the signal is converted into a high sampled pulse width modulated signal.

Figures 2.9 and 2.10 show the noise shaping in the frequency domain. As can be seen in 2.9, noise increases exponentially at higher frequencies. One important role of this step is shifting the noise to the higher frequencies to be able to remove it by applying a digital filter. The delta-sigma converter is a well suited for analog-to-digital conversion of low-frequency signals where high accuracy is needed.

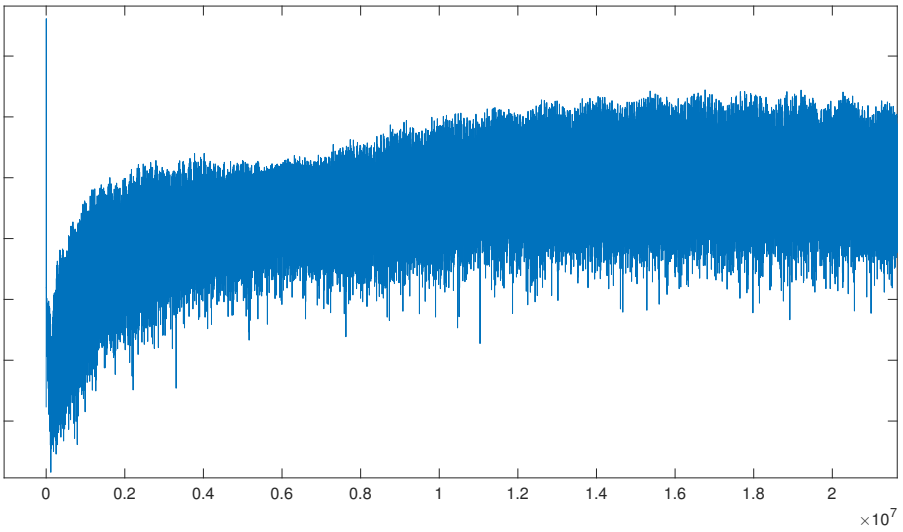

Figure 2.9: This figure shows representation of the signal power in frequency domain. As is shown, noise shaping is shifting noise in higher frequency, as a result, it can be removed by digital filters. This technique is suitable for signal in low frequency, since noise shaping reduces noise in lower frequency.

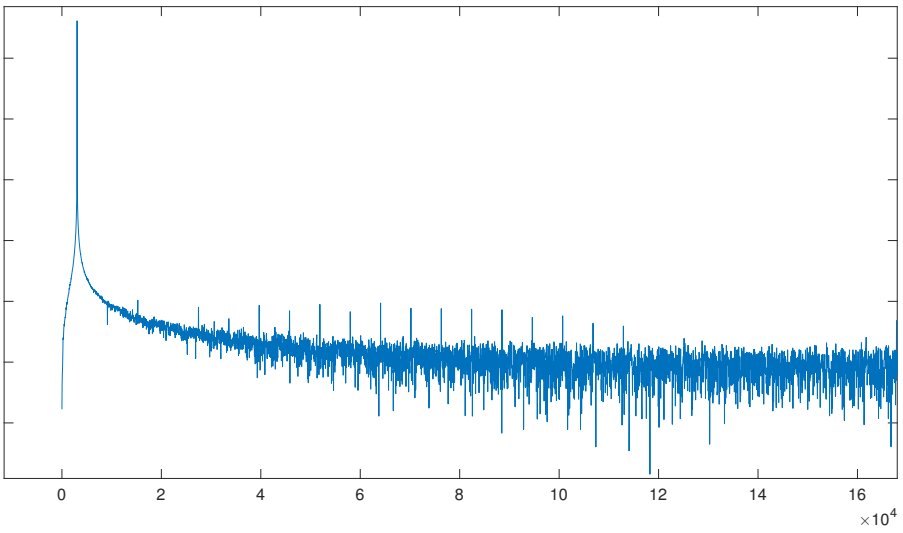

Figure 2.10: The figure shows a noise shaping behavior with more details in frequency domain. It shows that noise level in lower frequency is lower which can improve SNR. Noise in higher frequency can be removed by digital filter

The pulse-width modulated signal is converted to the digital domain with high-frequency noise as seen in figure 2.11. It can be seen that there is some noise due to quantization and modulation on the peaks of the signal, but it is filtered out by using FIR filters, as seen in figure 2.12 and figure 2.13 which results in the final digital output.

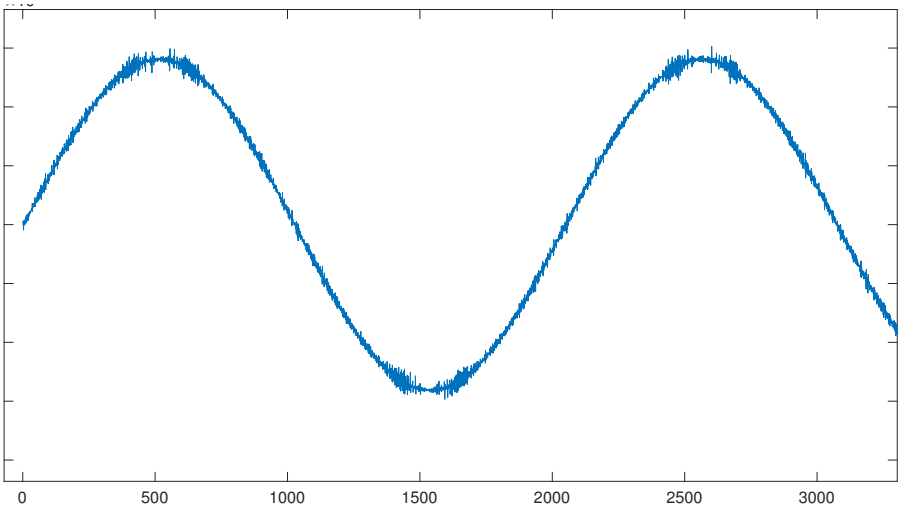

Figure 2.11: Digital signal within the Delta Sigma ADC without filtering which can be referred to as the signal after the Data Shifter block in figure 2.16

Two FIR filters are used to remove the noise in delta-sigma ADC conversion. Figure 2.12 and figure 2.13 show the digital converted signal in time domain. As it can be seen in figure 2.13, input signal is reconstructed with higher accuracy.

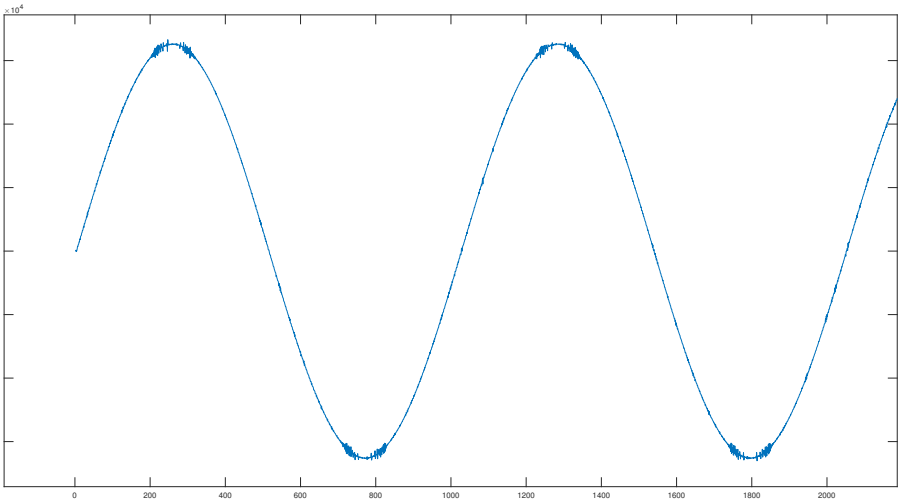

Figure 2.12: Digital signal within the Delta Sigma ADC with first FIR filter applied as showed as the first FIR filter in figure 2.16

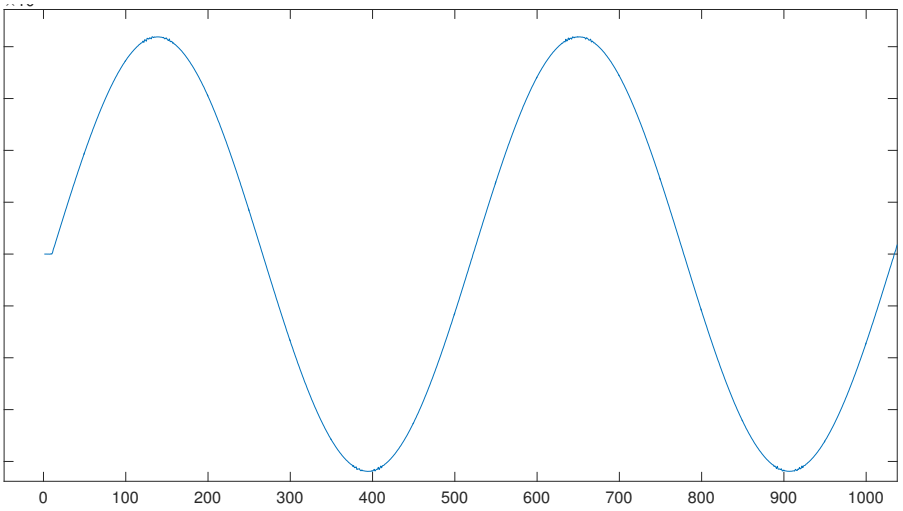

Figure 2.13: Digital signal within the Delta Sigma ADC with second FIR filter applied as showed as the second FIR filter in figure 2.16

2.4.3 Processor description

In this part, AURIX TC29x characteristics are explained[17]. AURIX is a new micro controller family produced by Infineon. This project is evaluated using Infineon Tricore family starter kits. The Tc29x has triple Tricore 32-bit CPUs up to 300 MHz, which support data memories, buses, interrupt system, direct memory access (DMA) controller and on-chip peripherals. Tc29x supports delta-sigma ADC with acceptable clock frequency, that is, tricore microcontrollers support delta-sigma ADC up to 20 MHZ.

Software Description

For implementing code into the TC29x Infineon's own AURIX software framework was used. The AURIX software framework is implemented in an Eclipse environment[19], which is a programming tool and integrated development environment. The software framework comprises software development tools and software objects. The software development tools are used to generate make-files depending on the toolchain compiler that is used to make the build executable, generate software source files and generate the operating system configuration. The process flow of the software development tools is shown in figure 2.14.

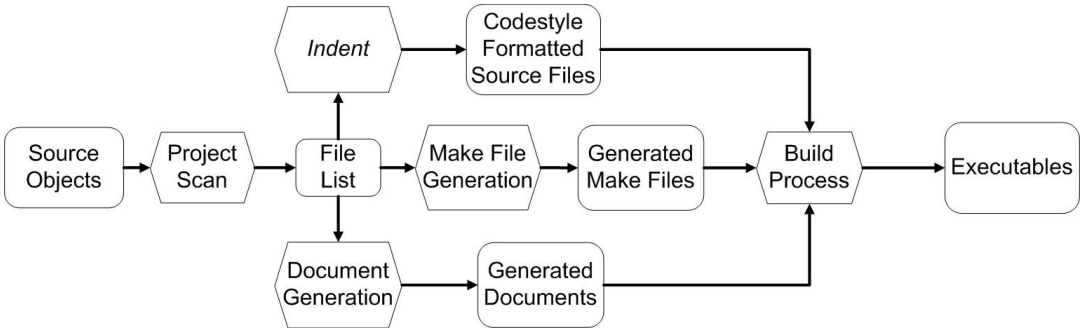

Figure 2.14: In the block diagram above is a representation of the process flow which the software framework is responsible for once the project is configured or built. It first scans the project and makes a file list. From the file list it uses a tool called Indent for code style formatting the source files. The software framework also in parallel generates documentation for the source files and make files for the chosen toolchain compiler which is used to build the executables.

The software objectives consist of application examples and function libraries for different modules that can be accessed on the TC29x. Among them is the delta-sigma ADC. The application example sets a baseline for the registers used by the specific module.

Hardware Description

The TC29x is a tri-core microprocessor with the three cores executing in parallel. However, for this thesis project, only one of the cores was used.

For this thesis project the module that is of interest to apply is the delta-sigma ADC module. There are several ways to access the delta-sigma ADC module in the TC29x: either through a peripheral bus directly to one of the cores or through other modules such as high-speed serial link (HSSL), bridge or direct memory access (DMA) modules and access to the cores can be achieved through a shared resource interconnect (SRI) crossbar. In this project we decided to have the connection directly through the peripheral bus. Direct connection made the implementation as fundamental as possible. Having a more complex implementation would result in the question if this was necessary or not.

In the delta-sigma ADC module there are internal clocks that can be used for sampling and interrupts. These clocks are unfortunately not fast enough for the precise timing that is needed in our application. Therefore, the Generic Timer Module (GTM) has been used to support the delta-sigma ADC to provide more precise timing. The GTM is also directly connected to the peripheral bus. The different connection paths from the used modules to the cores are shown in figure 2.15.

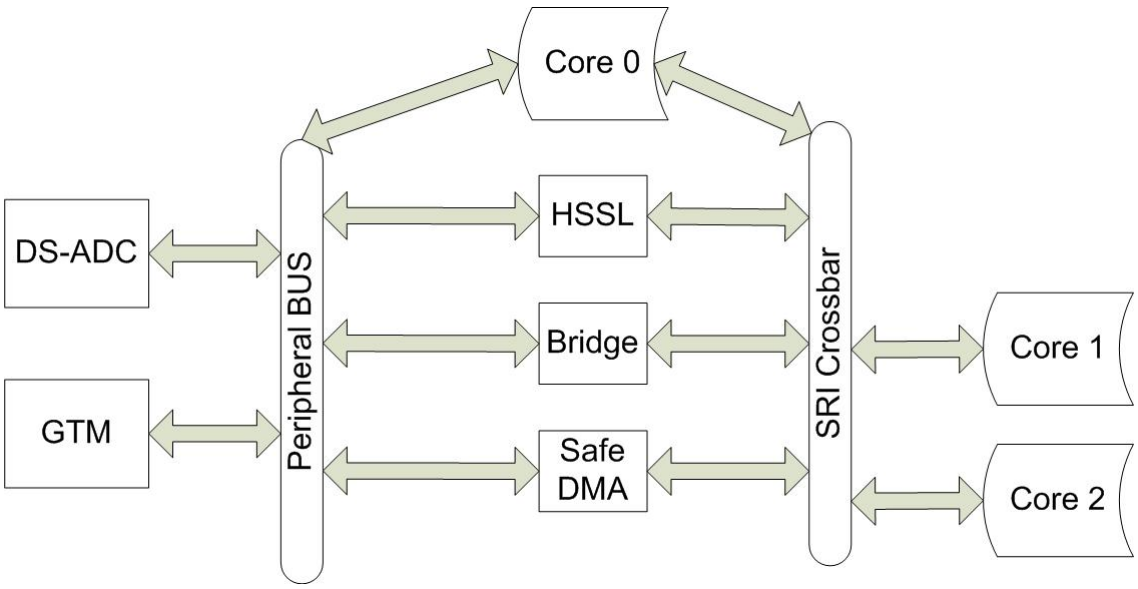

Figure 2.15: This figure shows a representation of the implementation options on how the delta-sigma and GTM modules can be implemented in the cores of the microprocessor. The most straightforward implementation, which was also used in this project, is to implement on Core 0 directly from the peripheral BUS. To gain access to the other cores the implementation has to be through either HSSL, a Bridge or a safe DMA. It could be necessary in the future to implement our measuring system in one of the other cores if many applications are used in the TC29x in the future. If so the implementation behind this project has to be changed.

Delta-sigma architecture

TC29x has number of inputs operating independently. Input pins can be selected by multiplexers. Also, each input pin has a choice of different channels that are programmable to it. The results of the delta-sigma ADC are stored in a specific register for each channel. Moreover, each pin can operate in two different modes: single-ended mode or differential mode. The delta-sigma ADC can work in two voltage ranges: 5 or 3.3 volts depending on the specific requirements. There are also programmable gain settings that can be used during the conversion: 1, 2, 4, 8 or 16. Delta-sigma ADC in TC29x can sample between 10 MHz and 20 MHz; high-performance and low-power modes are also available. Pass-band frequency in delta-sigma ADC of TC29x is between 10 kHz and 100 kHz. Since the frequency content of the rail pressure is below 50 kHz, the delta-sigma ADC meets the requirements in this project. In the demodulator, there exists filter chains consisting of one cascaded integrator-comb filter and two FIR filters with different coefficients. Figure 2.16 shows the different steps of delta sigma analog to digital conversion. It consists of analog fronted, the modulator and the demodulator.

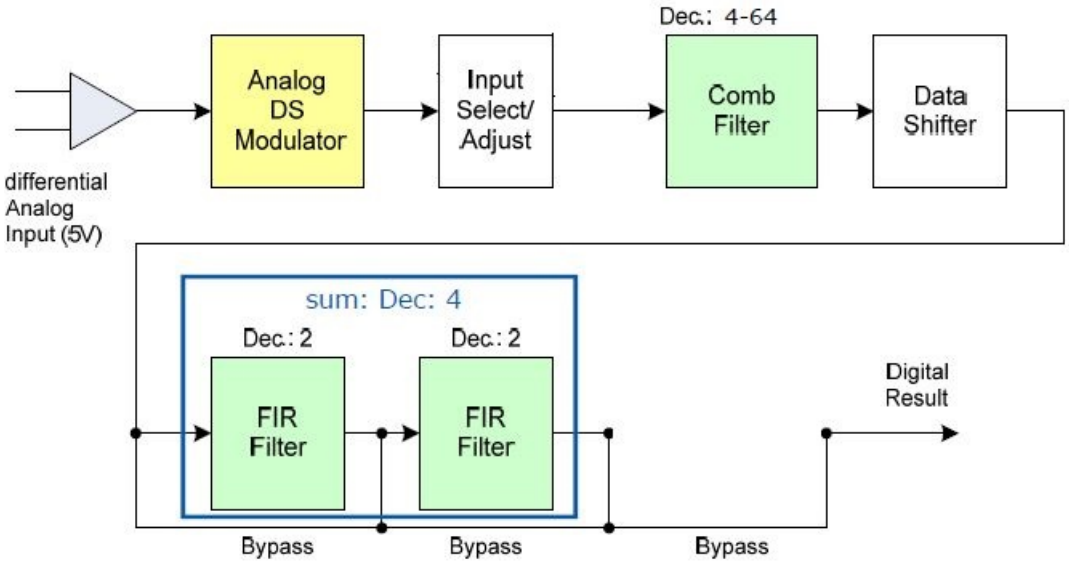

Figure 2.16: The figure shows delta-sigma ADC architecture. As is shown, the input signal is converted to PWM by the delta-sigma modulator. After that, the digital filter removes noise to achieve a higher accuracy. Two FIR filters can be used in this implementation with different characteristics. It is also possible to bypass the filters through the code. Finally, the digital results are stored in a register that is updated continuously.

As mentioned in section 2.4.2, the delta-sigma ADC has different orders. The data stream is converted from the analog input from pin by the on-chip 3rd order modulator. The decimation with selectable decimation rate can reduce the sampling rate of the input signals and FIR filters filter out the noise.

There exists an auxiliary filter to limit the converted signal. It limits the input by two limit values. This feature can save CPU performance and DMA bandwidth. Digital values are stored in registers. Results have 15-bit effective resolution for gain=1 and input voltage of 5 V. Result registers consist of 32 bits: 0 to 14 are used for results, bit 15 is the sign bit and 16 to 31 are reserved.

With different bandwidth and oversampling rate, SNR is changeable. It means that according to the application frequency, accuracy and SNR requirement, AURIX family can be configurable to achieve the set specifications.

3

Experimental Setup in Rig and Software Implementation

In this chapter we discuss the concept behind the injection rig used for data gathering and the importance of implementation and procedure of the data gathering.

3.1 Injection Rig

The injection rig provides an easily implemented environment for evaluation of engine performance. Since there are no pistons or crank stacks in the rig there is no possibility for combustion (see photograph of the rig in Appendix A.1). The fuel that would have been combusted is instead lead back to the fuel tank. In the injection-rig engine there is extra space that would normally have been occupied by pistons. This extra space provides additional opportunities of measuring and study the HP part of the injection system that would not be possible in an engine with pistons.

The rig has an interface directly connected to the ECU so that the engine performance can be set through parameters according to the engine-performance state. In our study we have chosen to look at the parameter settings of amount of fuel, revolutions per minute (rpm) and default rail pressure. These parameters influence other important parameters for our estimations, observed as visual data parameters such as rail temperature and the true injected fuel. The amount of injected fuel that is set in the ECU differs slightly from the actual fuel that is injected. The reason is that the injectors approximately inject the fuel amount that is set.

3.1.1 Scenario Set-up

To obtain measurements of common-rail pressure, scenario setups were made in an injection rig as presented in tables 3.1 and 3.2.

In table 3.1 five different scenarios are presented, in which each scenario was measured both with and without fuel being pumped into the rail after each injection. In the cases without pumping this refers in the first measurement that the fuel pumping has been turned off for two injections within the injection revolution. The parameters set in the ECU were chosen to characterize different cases depending on the load of the engine.

These measurements provided understanding on how the data should be handled and how to improve the data capturing.

The first set of measurements was made by using outlet metering valve (OMV) and nozzle control valve (NCV) as references for determining the pressure drop. The OMV supplied information about the fuel pumping into the rail and NCV supplied information about whether the injection needle was active or not.

Figures 3.1 and 3.2 show averaged signals of the rail pressure from cases from table 3.1. Figure 3.1 shows a case when the pumping was active (a normal condition case for an engine with one injection in the injection pattern). Marked green, in figure 3.1 show the pumping instances, which was later turned off. Marked pink, in figure 3.2 show where there is no pumping because of the switched-off pumping. As shown, the rail pressure remains constant when there is no pumping and when the next injection starts the rail pressure drops further.

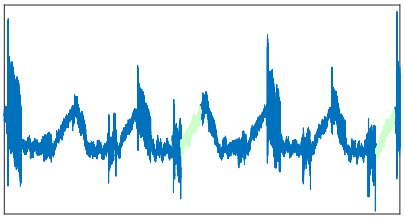

Figure 3.1: Above is a presentation of the averaged rail pressure of case 1, table 3.1. The case represents a scenario where all pumping is active and can be seen over one entire injection period (duration for when all six injectors have been active). The green marking represents the pumping occasions in which was later turned off in case 2 (presented in Figure 3.2.

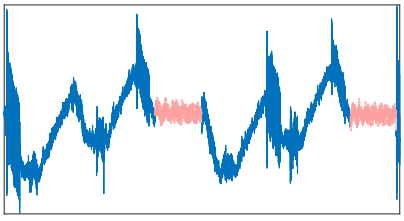

Figure 3.2: The graph above shows the averaged rail pressure of case 2, table 3.1. The case represents the same scenario as Figure 3.1 but with the pumping turned off in two occasions which are presented in pink color.

Table 3.1: This table represents the first measurements setup in the injection rig were the measurements were made both by having all pumping turned on and with some pumping occasions turned off. These cases were not included for any results but are used for theoretical descriptions in this project.

Cases:	1	2	3	4	5	6	7	8	9	10
With or without pumping	With	Without	With	Without	With	Without	With	Without	With	Without
Engine Speed (rpm)	1800	1800	1200	1200	800	800	800	800	1800	1800
Set rail pressure (bar)	1000	1000	1600	1600	2400	2400	2400	2400	1000	1000
Set fuel amount ($\frac{\text{mg}}{\text{stroke}}$)	200	200	100	100	50	50	200	200	200	200
Actual fuel amount ($\frac{\text{mg}}{\text{stroke}}$)	197.7	197.7	101.7	102	46.8	48.3	200	Not Possible	197.3	197.3
Rail temperature (Celsius)	87.5	86.7	94.6	98.9	110.4	123.7	125	Not Possible	92.6	89.6

Table 3.2: The table below represents the redone measurements made with a split adapter to reduce the noise within the measurements obtained in table 3.1. The measurements in this table were done by having the pumping before the injection of interest turned off in all cases. As an outcome of reducing the amount of measurements in contrast to table 3.1 additional fuel amounts were added. The additional fuel amounts could be represented as just having one main pilot injection.

Cases:	1	2	3	4	5	6	7	8	9	10	11	12
With or without pumping	Without	Without	Without	Without	Without	Without	Without	Without	Without	Without	Without	Without
Engine Speed (rpm)	1800	1800	1200	1200	800	800	800	800	800	800	800	800
Set rail pressure (bar)	1000	2400	1600	2400	1000	2400	2400	2400	2400	2400	500	500
Set fuel amount ($\frac{\text{mg}}{\text{stroke}}$)	100	200	100	250	50	100	200	220	3	5	5	3
Actual fuel amount ($\frac{\text{mg}}{\text{stroke}}$)	98	196.7	96	240	49	98	189	210	2.4	4.4	4.8	2.8
Rail temperature (Celsius)	93.8	112	99.4	111.7	95	115	121	118	108.3	100	90	87.8

As can be seen in figure 3.2, when the pumping is turned off before an injection it is much easier to locate the pressure drop. This localization in figure 3.1 would not be possible without knowing the localization of NCV or SAC. However, figure 3.2 show injections at different pressure levels and to determine the decay and target pressure is very difficult. This was not a desired scenario, since there is no structural variance within the signal. It can be seen that after the first injection in figure 3.2 there is a variation of decrease for the different injections and the variety of pressure levels became very confusing. Because of this and that these measurements are much too noisy (explained in section 3.1.2) it was decided to redo the measurements and make sure that the pumping was only turned off before the injection of interest and at no other time. In the next measurement setup, as seen in table 3.2, all measurements were done without pumping during the injection from the injector which was selected to be investigated. In figure 3.3, two crank revolutions are shown. Figure 3.3 starts with the injection from the injector of interest and ends with the pumping turned off for this injector. The pink marking shows the lack of pumping before the injection of interest.

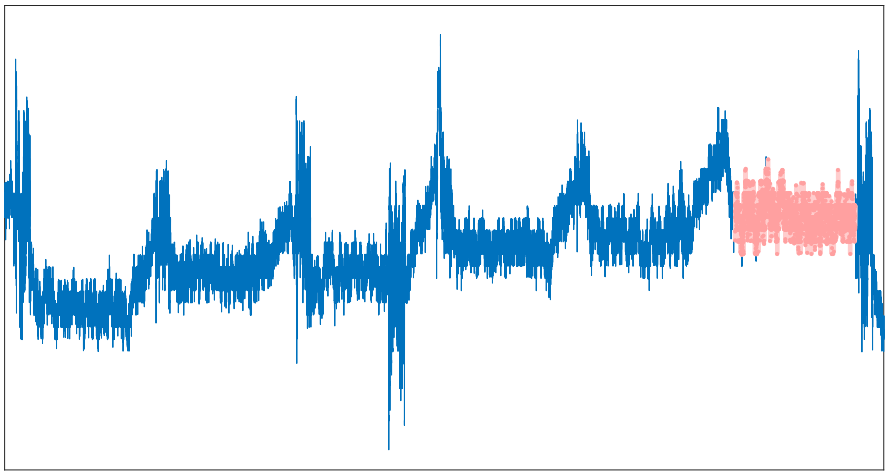

Figure 3.3: The graph shows one entire injection period for a case from table 3.2. The pumping in these cases has been turned off before the injection of interest is activated. This lack of pumping is marked in pink at the end of the period of the injection in the graph.

The second measurement setup was made with additional cases than in the first measurement. These cases were added to obtain more variations in injected fuel amount. In a normal case scenario, where the injection contains pilots (pre injections), the quantities will be as low as 3 to 5 mg/stroke.

3.1.2 Noise reduction in measurement setup

Since the first measurement study showed some undesirable qualities in noise and pumping sequence, the measurements were re-executed to reduce noise and disturbances. It is known that there is noise in the rail-pressure signal that would be possible to filter out. However, if the data contain a high amount of noise, filtering could destroy the signal. To not risk this it was decided to redo the measurements with cases and settings as described in table 3.2.

It appeared that the main noise source was a break-out box connected between the sensor and oscilloscope. To solve this problem, the rail-pressure sensor was instead connected directly to the oscilloscope by a split adaptor. Figure 3.4 shows the noisy signal obtained in the first measurement setup and figure 3.5 shows the measurements by utilizing the split adaptor.

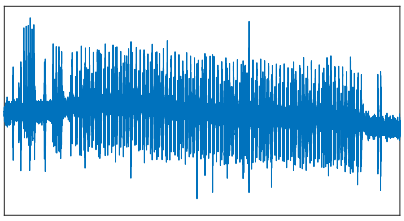

Figure 3.4: The graph above shows a duration of one injection from table 3.1 for when the break-out box was used. It can be seen that the signal consists of a lot of high frequency noise, which is not desirable. Even if the signal would be filtered the uncertainty of filter away necessary data can not be neglected.

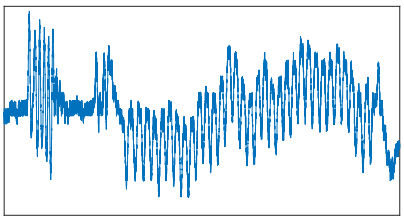

Figure 3.5: Above is a representation of the injection duration using the split adapter which was used for the second measurement setup presented in table 3.2. It can be seen that the signal does not contain the noise as shown in figure 3.4 and a much cleaner signal is measured.

As can be seen from figures 3.4 and 3.5, data from measurements became less noisy. The main benefit of having this adaptor is that the external filter is not needed anymore. Less hardware makes it easier to capture the data and filter effects such as latency, complexity and component effect will be cleared out.

3.2 MATLAB and Simulink Evaluations

In this section, a general picture of data processing will be discussed for MATLAB and Simulink.

3.2.1 Signal adjustments for processing

Data from the test rig are stored in an oscilloscope and need to be imported into MATLAB for analysis. Files from the oscilloscope can be copied to the computer, but they can not be imported to MATLAB directly. To solve this issue, a function (called reader) can be used. Since this file has different recorded data, it needs to be separated as well. In this case, recorded data consists of rail pressure , SAC, NCV and OMV signals. When data are imported to MATLAB, they are saved into a mat file with one group and 4 traces. Reader function separates the data into different variables. As the function separates the data it creates time lines for the imported signals according to their sampling rate frequencies. Later on, this time line is very crucial to estimate quantity of the signals. However, since the recorded data have all the same sampling rate this did not become an issue. As a result, time for our measurements is in the right order when the correct values are achieved for the different sample steps.

Since the rail-pressure signal has a noisy characteristic, it is necessary to adjust the data before executing any processing evaluations. This is done by implementing a smoothing function. This smoothing function calculates an average of a constant number of samples in comparison with the surrounding samples. The form of the signal can be changed and simplified as shown in figure 3.6.

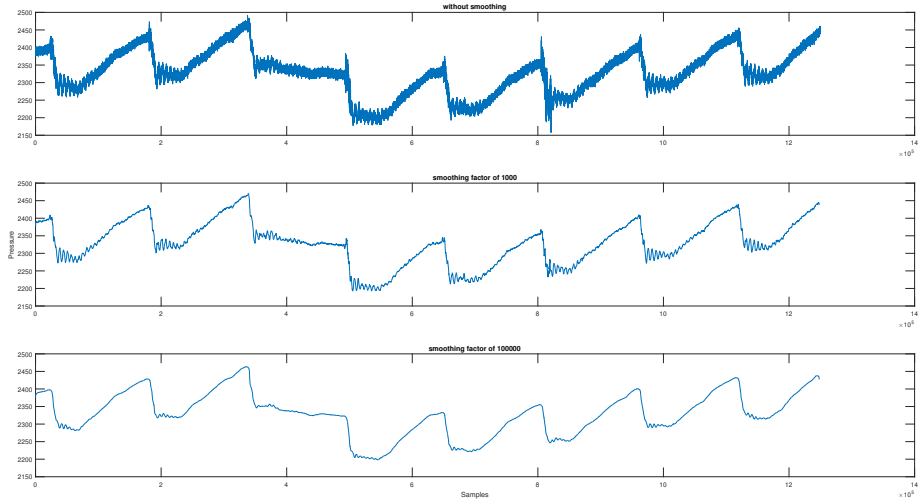

Figure 3.6: The figure shows a representation of the process of using the smoothing filter. The top graph shows the rail pressure signal without any smoothing filter applied. The graph located in the middle shows the signal with the smoothing filter using 1000 samples and the bottom graph shows the signal with the smoothing filter using $100,000$ samples. It can be seen that by applying the smoothing filter the signals undesired high-frequency content can be removed without destroying the characteristic of the signal.

3.2.2 Simulink model

Once the data have been adjusted and converted into a time-series variable, the Simulink model can be executed. As is shown in figure 3.7, the delta-sigma ADC uses three first-order ADCs cascaded together with filter chains to reduce noise and gain higher accuracy. This technique is called multi-stage noise shaping conversion[9]. The filter chain has two filters which are FIR with different characteristics. Finally, an integrator measures an average and stores it in digital results. These first-order ADCs run in linear mode. As is shown, a MASH model is used in this simulink model during simulation.

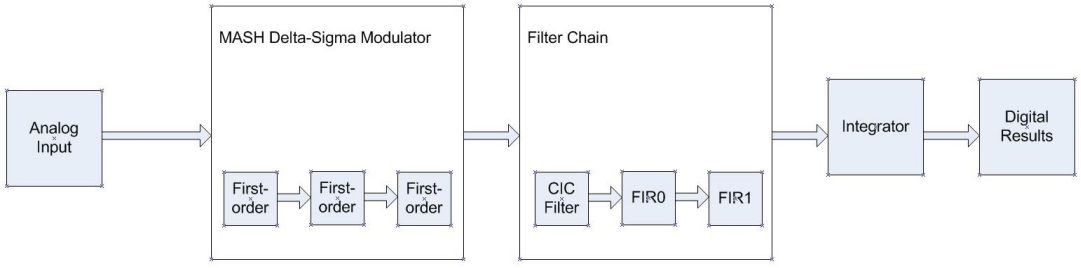

Figure 3.7: The figure shows the Simulink block diagram of the delta-sigma ADC which is used in this implementation.

After the model has been executed for a period of the injection, a digital result will be stored in the MATLAB workspace. For detecting the pressure variance during the injection an additional MATLAB-function has been used.

3.2.3 Pressure Drop Detection

As mentioned in section 2.3, when the injection starts the common-rail pressure will drop sharply. By detecting the common-rail pressure in the MATLAB implementation, the delta pressure can be estimated. Meanwhile, the amount of injected fuel can be calculated through equations (2.2) and (2.3) since all parameters are known for our measured cases.

3.2.4 Temperature Model

As mentioned previously in section 2.3, the estimation of the injected amount of fuel is highly sensitive to temperature changes. During the measurements, the fuel temperature was monitored by the injection rig. However, outside the injection rig, in an actual engine, the fuel temperature is estimated through parameters which have been evaluated by a Simulink model. Therefore, it is highly important that the Simulink model is calibrated correctly to give a true and realistic temperature estimation through the used parameters. By having an accurate estimation, it is possible, through calculations, to obtain a fuel consumption close to the real injected amount.

The temperature estimation model is a Volvo proprietary Simulink model, which uses parameters that are measured in the engine and by using dependencies estimates the temperature for certain conditions. Since the dependencies can vary between conditions, the calibration is significant to avoid contribution to errors in the temperature estimation.

By using the settings of the different measurement scenarios shown in table 3.2, into the temperature estimation model together with ambient calibration parameters, the temperature for each scenario can be estimated.

The scenarios do however contribute to a bigger problem. Changing operating conditions will create temperature changes as well. It is not even guaranteed that the temperature will stabilize before the operating condition changes again. It would therefore be significant to measure temperature variation, specifically during the injection duration. If this is done using the same sampling frequency and timing as for the rail pressure, the same procedure as for estimating the pressure drop could be implemented for the temperature signal.

It is also important to be aware that the temperature model uses only target pressure and engine speed (RPM) together with additional engine compartment characteristics. Additionally for this the model is calibrated to satisfy scenarios for an engine with a combustion system and engine compartment as shown in figure 3.8. Temperature estimation will give a significant error for the temperature. However, because this is a property of specific engine installations, different engine setups will provide a difference in temperature compared to the injection rig. When using estimation versus the measured temperature the error will differ due to variation of the set conditions. This is a trade-off which has to be further investigated and have a proper temperature determination.

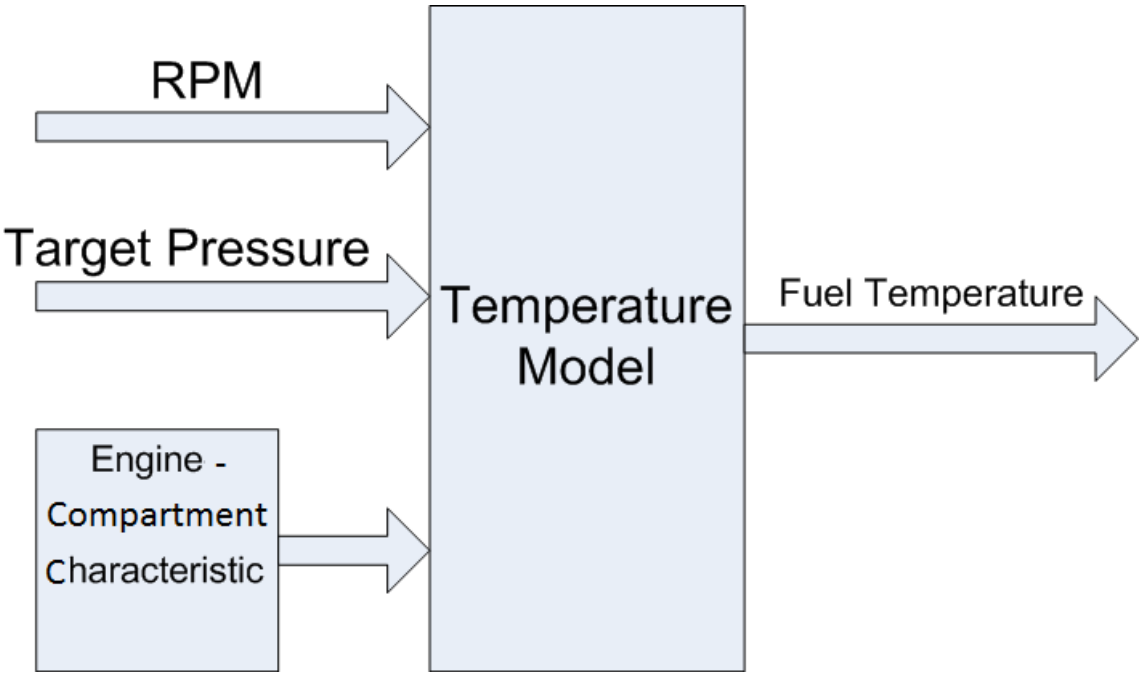

Figure 3.8: Shown above is a black-box representation of the fuel-temperature-estimation model. Because of the confidentiality behind this model only the common parameters behind our measurement setup and the model are presented as the engine speed (RPM) and the target pressure. The box of Engine Compartment Characteristic will remain unknown in this report.

4

Implementation of Delta-Sigma ADC

How to estimate injected fuel amount from rail pressure by pure calculations is previously described in chapter 2. However, to estimate the amount of injected fuel by sampling the rail pressure in real time, the accuracy is of a much higher significance than for the MATLAB evaluation.

This chapter will discuss the implementation of the delta-sigma ADC and the estimation of the amount of fuel with real-time sampling. The implementation has been done using a desk setup and later tested in the injection rig.

4.1 Realtime Implementation of Delta-Sigma ADC

In an engine the fuel injections for optimizing emissions operate in real time. It is therefore desired to be able to estimate the injected fuel amount to see if the engine optimization is actually as good as desired. It is also useful to know if all injectors are working or if there is leakage in the injectors. Because of this, a real-time implementation of our fuel estimation has to be implemented. The implementation will give results of how well the rail pressure can be sampled, which has a significant role in how small amounts of injected fuel can be detected.

The real-time implementation to the Infineon evaluation board has been done on a desk setup using listed equipments (see photograph of setup in Appendix A.2):

- Project board
- Quad Operational Amplifier
- Function Generators
- Voltage Supplier
- Infineon evaluation board
- Eclipse Compiler

4.1.1 Analog Simulations of Rail Pressure

Our project had limited access to the injection rig, since the rig has to be used for other projects. To do the evaluation with the Infineon evaluation board would not be possible due to working conditions and maintenance of the injection rig. Because of these circumstances the rail pressure had to be simulated somehow for the desk setup. As can be seen from the MATLAB implementation in chapter 3, the rail pressure signal had specific characteristics in appearance. The rail-pressure appearance is a half-wave rectified sinusoid upon a ramp function. This appearance can be simulated by using two function generators, one set to a sinusoid function and the other to a ramp function. The sinusoid function is sent through a diode which cuts the negative voltage and later sent to an adder implementation of a operational amplifier where it is combined with the ramp function, as shown in figure 4.1. This emulation of the rail-pressure signal can be connected to the differential pins of the evaluation board.

Figure 4.2 shows the rail-pressure signal recorded from test rig and figure 4.3 shows the signal simulated by the rail-pressure emulation. It is possible to adopt the signal by changing the amplitude and frequency to have it more similar to the different scenarios. As is shown in the figure 4.3, the simulated signal does not have any noise. It is also possible to add noise by connecting another function generator to the circuit to produce noise (low amplitude with high frequency), but in this project, the rail-pressure signal without noise is used.

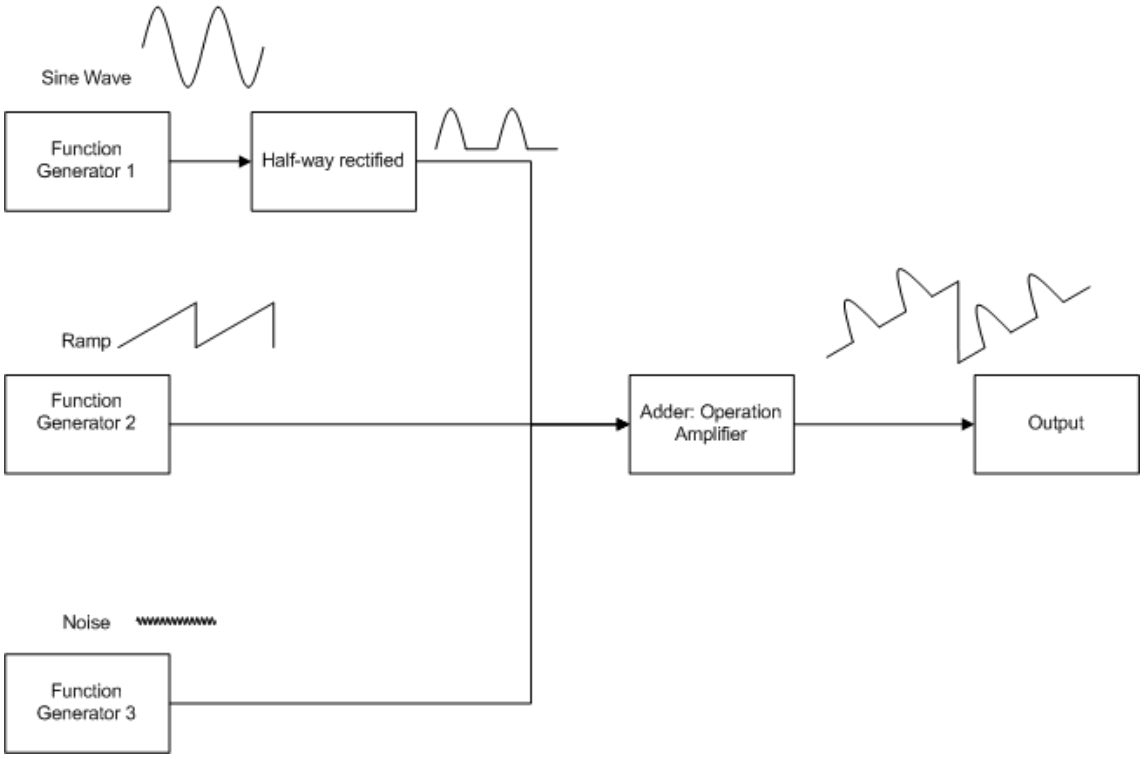

Figure 4.1: Shown above is a block diagram of how the rail pressure was emulated. As can be seen the first function generator generates a sinusoid wave, which is half-way rectified. The half-way rectified wave is later added together with the second function generator, which generates a ramp function. Using an operation amplifier the result shows a good representation of the graph in figure 3.6. The emulation could also add an additional function generator to simulate a noise characteristic, but was not implemented.

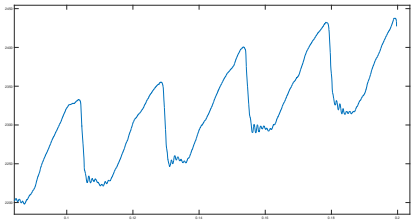

Figure 4.2: The graph above shows the rail-pressure signal as presented in figure 3.6.

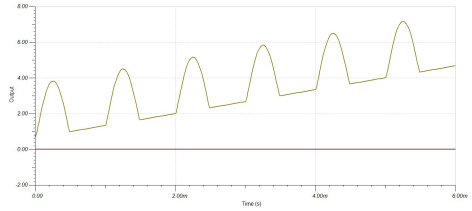

Figure 4.3: Above is a representation of the simulated rail-pressure signal described in figure 4.1.

In addition to having function generators to simulate the rail-pressure signal, a pressure sensor was connected to the differential input. In this implementation, a pressure pump was connected to the pressure sensor. The pressure was then pumped up to a certain value and after release back to zero. The aim of having this test is to check that the circuit is working with a real sensor in real time before the final execution in the test rig. Since the result of this test is not scientific, it is not covered in this report.

4.1.2 TC29x Delta-Sigma ADC

In this section, a brief description of the hardware implementation of the delta-sigma ADC will be discussed. Delta sigma ADC is implemented in one of the three available cores. To be able to execute delta-sigma conversion on the Infineon board, some registers must be set and enabled. Some important registers which need to be set are: clock source, clock frequency, decimation factor, filter type, supply voltage, input pins and channel, sample frequency. These registers will be set according to the specification. In this implementation, one input will be converted to digital, by assigning the negative pin of the differential mode to ground, only the positive pin in the differential mode will be used as input. It means that the input signal has to be connected to two pins: positive input to sensor and negative input to ground due to the differential mode.

Another important part of the implementation is the generic timer modulator(GTM). Since high accuracy is very important in real time, GTM has to be implemented. To be able to use the GTM, some registers need to be set as well. Period, duty cycle, internal path and trigger controls will be set.

Moreover, trigger is vital to control the sampling and delay. Trigger for the delta-sigma ADC has its own register and peripheral connection. The number of samples in each interrupt can affect the CPU efficiency, DSP unit and memory. In this case, a constant number of sample points will be stored in each interrupt, sent to the DSP function and return the pressure gap in each injection.

To achieve the possibility to read values between certain points in time, there is a register which controls the timestamp which might be possible to use in this project according to the constant time between each injection. But in this project, the timestamp was not used for this purpose.

Total delay of conversion can be easily calculated according to the data sheet. The total delay can be calculated by as:

$$Delay = [7 + 1 + (\frac{3 \times (N-1)}{2}) + (3.5 \times N) + 3 + (27 \times N) + N + 5] \times T, \quad (4.1)$$

where N is the oversampling rate and T is $\frac{1}{Fs}$. In this project, since $N = 32$ and the sampling frequency, $Fs = 20$ MHz, total delay is:

$$Delay = [7 + 1 + (\frac{3 \times 31}{2}) + (3.5 \times 32) + 3 + (27 \times 32) + 37] \times \frac{1}{Fs} \quad (4.2)$$

Which gives us:

$$Delay = (7 + 1 + 46.5 + 115 + 901) \times 50\ ns = 53.525\ \mu\text{s} \quad (4.3)$$

Since the pressure sensor which is used to obtain the rail-pressure signal has a response time of 15 ms this delay is not an issue when obtaining the measurements.

Finally, the result of the delta-sigma ADC is stored in a register. This register updates continuously, then it needs to be saved in another register to be stored and processed. The digital result consists of 14 bits resolution; moreover, accuracy of this conversion is very high. The analog signal converted to digital is saved in a register. To be able to convert the result to the signal value, the result's constant floating number has to be multiplied to have a digital result. For example, when the converter connected to 0 V, "0000000000000010" was stored in a register which stands for "2" in decimal. Moreover, maximum signal can be converted to digital is 5 V. The digital result of the conversion is "0010101010111011" which stands for "10939" in decimal. This constant factor was calculated as 0.00045716.

As can be seen, 14 bits represent the digital result of the conversion. Other analog inputs between 0 and 5 V have a digital value in this range. By having the number of bits, it is possible to convert the binary value to digital values.

There are two functions beside the delta-sigma ADC: Average calculator and pressure gap finder. Average function or mean function calculates the average value of the signal values by using the certain number of points. Dependent on the signal characteristics, the number of points can be changed. The aim of this function is removing the noise from the signal. As shown in section 3.2, the median filter can clear the signal from unwanted noise.

The last function is finding the critical point of the signal. It means that a certain number of samples will be compared to each other to find the pressure drop in injection. To be able to do this, one injection period has to be converted to digital, saved to the memory and analyzed. By adding a very short delay, one period of injection can be stored in an array. Therefore, this array can be imported to the function and analyzed by a comparator. As a result, this function returns the pressure drop in each injection. The most important part of this stage is finding the right number of samples to be able to capture the whole period of injection, since the injection is periodic and it is repeating in a constant time.

4.2 Real-Time Implementation in the Injection Rig

Even if the results from the desk setup gave good results the specific parameters for fuel estimation were not available, except for the pressure drop. Therefore the evaluation board together with the delta-sigma implementation was taken to the injection rig setting up several real case scenarios. The scenarios that were implemented contained a full injection pattern with pilot and main injection. By these implementations the pilot was set to 5 mg/stroke with varieties of main injections of 20, 100, 200, 360 mg/stroke. To perform worse scenarios also the target-rail pressure was changed between 700 bar as a low working condition and 2400 bar as a high working condition.

5

Results and Discussion

In this chapter, the results of the different implementations are presented; in MATLAB and AURIX evaluation board (real-time implementation). The two implementations convert the rail pressure values for the significant measurements and use different strategies for determining the pressure drop that can be used for the fuel estimation.

5.1 Result of MATLAB and Simulink

The measurements used for obtaining the results in the MATLAB implementation are shown in table 3.2. In these measurements, the SAC pressure was accessible during the simulation. However, the SAC pressure is not available in an engine with combustion cylinders. It is important to be aware of the delay between the NCV signal and the injector SAC pressure as shown in figure 5.1. If the implementation uses the NCV signal for the fuel estimation, this delay will influence the detection of the rail-pressure drop during the injection. It means that by having the delay, maximum and minimum points will be shifted right and since the slope of the signal is very steep, a huge error may be added.

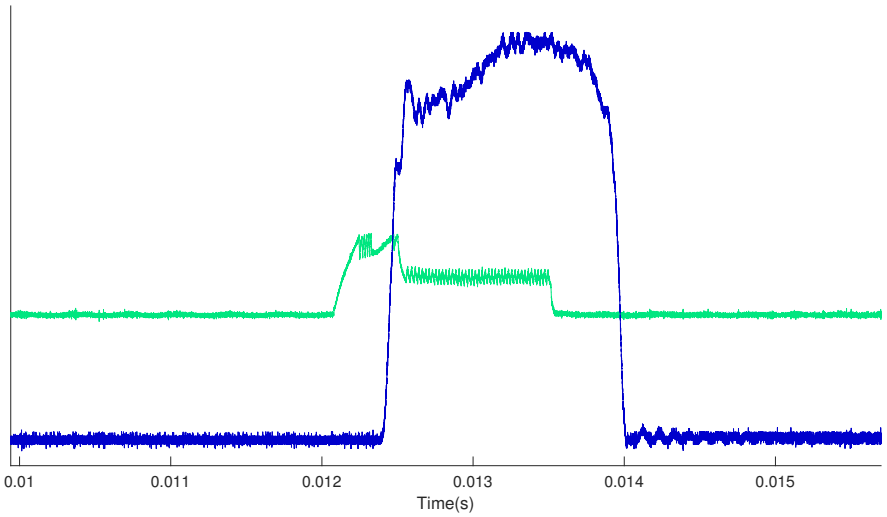

Figure 5.1: The graph above presents the NCV in the green curve and the SAC in the blue curve with higher amplitude throughout time. It can be seen that the NCV has the same duration time as the SAC but with an introduced delay. Once the NCV opens the needle valve fully the SAC pressure will increase. The delay can therefore be seen as the time the valve is opening.

Figure 5.2 shows the rail pressure and SAC pressure. It can be seen that the pressure drops accordingly when SAC pressure is active. In the measurement setup the implementation was to turn off the fuel pumping after the investigated injector. Therefore , a noticeable drop can be seen during the time SAC is active. This will clear out any disturbances of pumping influence, making it easier to locate the stop of injection.

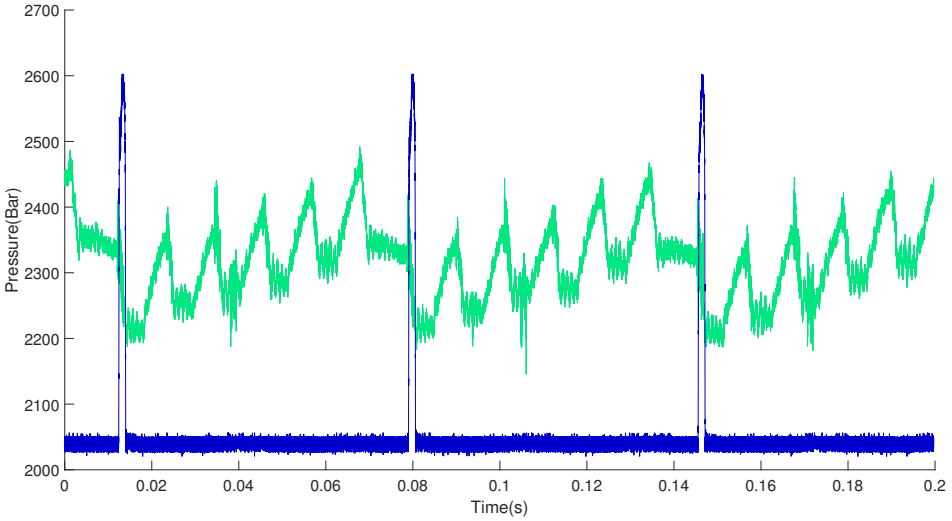

Figure 5.2: The graph above shows the rail pressure and SAC pressure. In this figure there are three injection periods and the SAC pressure of the injector of interest is active three times. The rail-pressure drop within these activations of SAC is the pressure drop during the injection, which is referred to as ΔP.

In a zoomed image of the injection shown in figure 5.3, it can also be seen that the rail-pressure starts to fluctuate at higher frequencies some milliseconds before the SAC pressure is active. This is a result of that the NCV activates the nozzle and the fuel gains access to the injector. However, the fuel is not injected to the cylinders until the SAC of the injector has reached a certain pressure. It can also be seen that the higher frequency fluctuation is stabilized a bit before SAC is lowered. This is a result of that the NCV is no longer active but as can be seen, there is still SAC pressure and fuel is still injected into the cylinders.

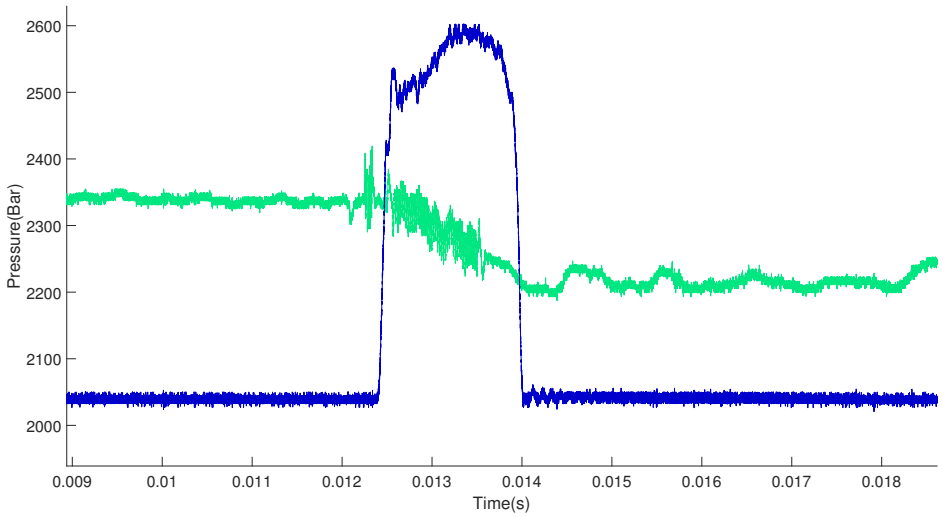

Figure 5.3: Above is a zoomed-in case of an injection from figure 5.2. It can be seen what duration the SAC pressure holds and therefore also the duration of the pressure drop (ΔP).

5.1.1 Case specific results

By applying the smoothing filter to the rail-pressure signal, the noise disturbances and higher frequency contents are canceled out. The rail-pressure values can then be read in a much more precise manner.

In figure 5.4, the smoothed rail pressure is presented with the pressure drop detection. As shows in table 5.1, case 1, the set target pressure for this case is 1000 bar.

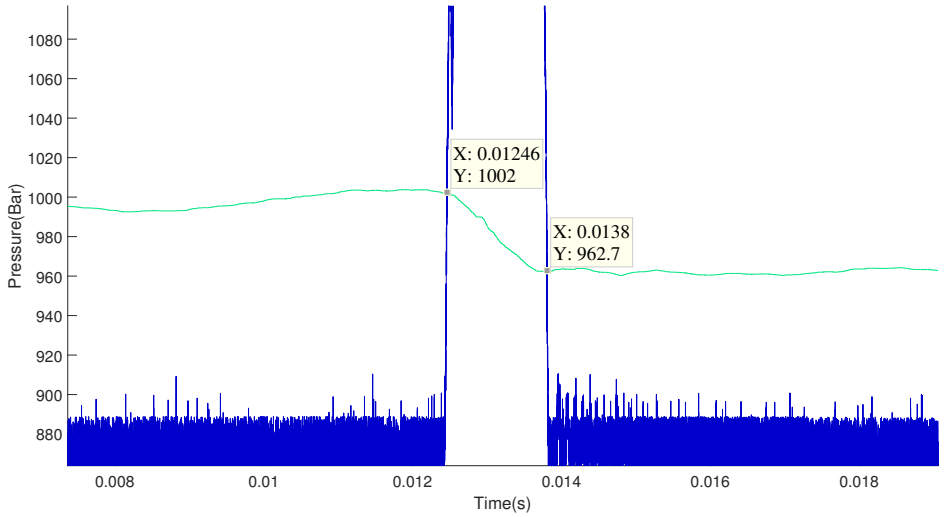

Figure 5.4: The graph above shows the representation of figure 5.2 for case 1 from table 3.2. The point of the pressure drop is also shown above as the pressure drops from 1002 bar down to 962.7 bar.

It can also be seen in figure 5.4 that the pressure drops around 38.4 bar. From this, the fuel can be estimated as presented for case 1 in table 5.1.

Consider case 3 presented in table 3.2, the target pressure is set to 1600 bar. This can be seen in figure 5.5 in the same manner as for figure 5.4. However, an interesting result is that the pressure drops by 45 bar during the injection even though the same amount of fuel is injected as for the first case (presented in figure 5.4). One reason for this is the high target pressure contributes to a smaller fuel-volume density in the rail. Hence, injecting the same amount of fuel under a higher target pressure corresponds to a larger volume quantity.

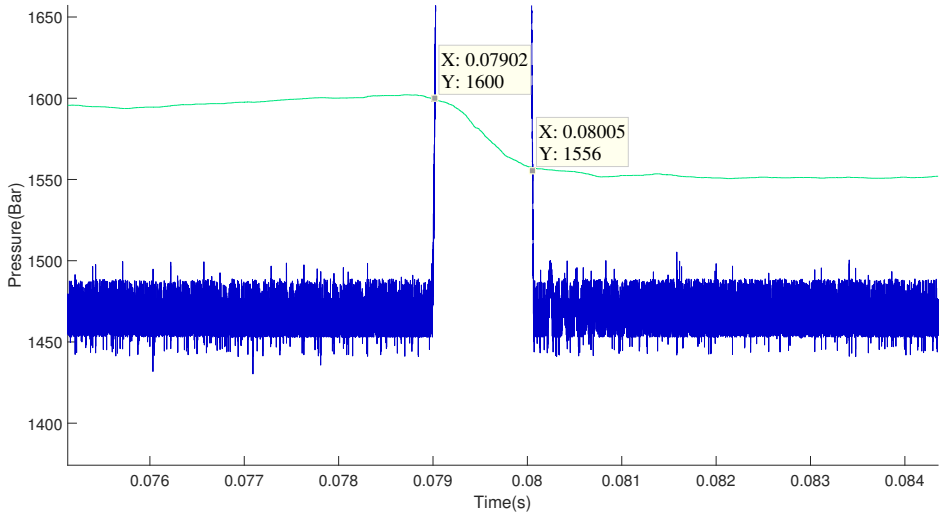

Figure 5.5: The graph above shows in the same way as figure 5.4 the representation of figure 5.2 for case 3 from table 3.2. The point of the pressure drop for this specific case are also shown above as the pressure drops from 1600 bar down to 1556 bar.

The same result is further shown in figure 5.6 where the target pressure is set to 2400 bar (see table 3.2). The pressure drops even at a steeper rate of 97 bar than previously, even if for case 1 and case 3 have the same amount of injected fuel.

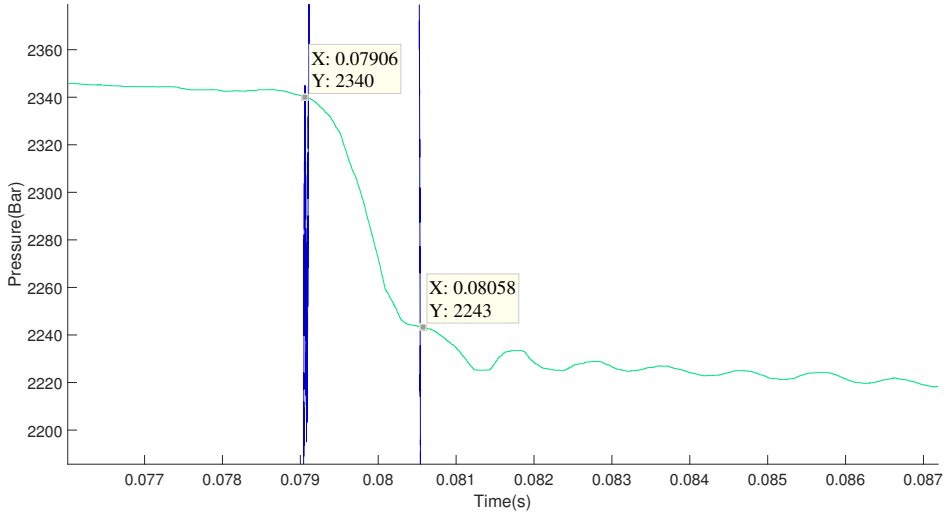

Figure 5.6: The graph above shows in the same way as figure 5.4 and figure 5.5 for case 6 from table 3.2. The point of the pressure drop for this specific case is also shown above as the pressure drops from 2340 bar down to 2243 bar.

Consider case 2 presented in table 5.1, the target pressure is set to 2400 bar and instead of injecting 100 mg/stroke, 200 mg/stroke is injected. It can be seen in figure 5.7 that the pressure drop is 103 bar, which is very close to case 6.

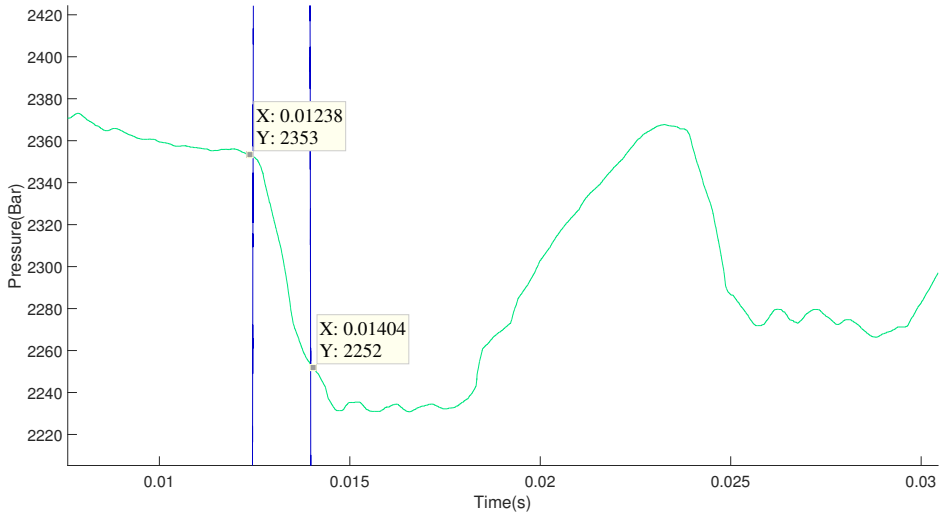

Figure 5.7: The graph above shows in the same way as figure 5.6 the representation of figure 5.2 for case 2 from table 3.2. The graph is a bit zoomed-out in contrast to figure 5.4, figure 5.5 and figure 5.6 as can be seen in the time-axis. The point of the pressure drop for this specific case is also shown above as the pressure drops from 2353 bar down to 2252 bar.

Table 5.1: The table presented below shows the monitored actual injected fuel presented in table 3.2, together with the cases implemented in MATLAB for estimating the injected fuel. Both the monitored values and estimated values are presented in mg/stroke. The notification *ERROR* represent values which were not able to be estimated by the MATLAB implementation.

Case	Actual Injected Fuel Amount mg/stroke	Estimated Fuel Amount mg/stroke
1	98	114
2	196.7	178.5
3	96	93
4	240	240.9
5	49	34.9
6	98	84.1
7	189	180.1
8	210	211
9	2.4	*ERROR*
10	4.4	*ERROR*
11	4.8	*ERROR*
12	2.8	*ERROR*

In the MATLAB/Simulink implementation the temperature is known and the amount of injected fuel can be estimated as described in section 2.3. These results are presented in table 5.1. The table shows the monitored values of the actual injected fuel in the different cases presented in table 3.2 together with the fuel estimation. It can be seen that the fuel estimation shows promising results and is more accurate with larger amount of injected fuel. However, there are some differences between the injected and estimated amount. These are believed to be due to the uncertainty in the bulks modulus. However, the results are within an acceptable range. The table also shows errors for the small injections between 2 and 5 mg/stroke. These are due to the noise distortion and the implementation fails to detect the pressure variance during this small injection. From this error it can be stated that the MATLAB implementation is not able to detect a pre- or post injection.

5.1.2 Temperature investigation results

As mentioned in section 3.2.4 there is currently no temperature sensor in the engines to measure the fuel temperature and an estimation model is used instead. Since this model is calibrated for a system with a combustion chamber it is expected to differ from our measurements which are executed without a combustion chamber. However, since our results are all obtained in the injection rig it is highly significant to be aware of any differences that are to be expected when implementing onto the ECU and having the control on an actual engine. In figure 5.8, it can be seen that the temperature model used on the ECU is overestimating and underestimating the different cases presented in table 3.2.

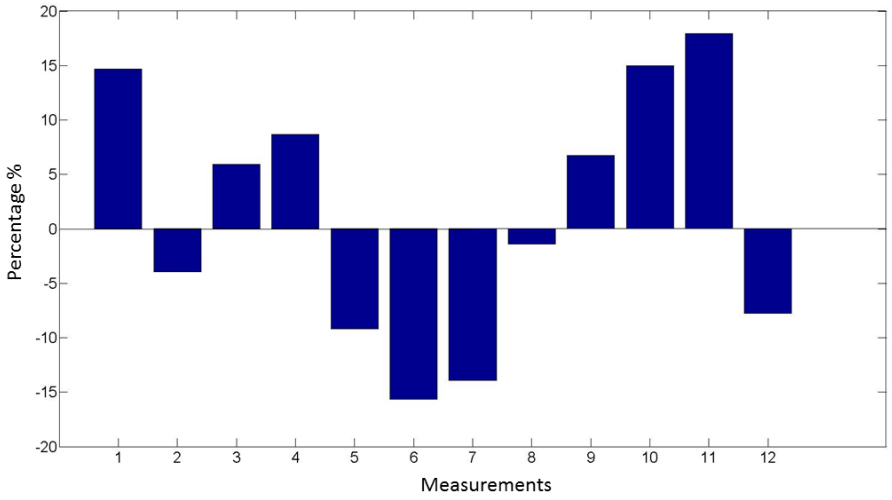

Figure 5.8: Above is a representation of the overestimation and underestimation percentages between the estimated temperature model described in section 3.2.4 versus the monitored temperature presented in table 3.2 for the twelve different cases. The target pressure and engine speed was set into the temperature model (see figure 3.8) for each case and compared with the monitored value of the case in table 3.2. For positive percentage values the model has overestimated the temperature.

There does not seem to be any correlation between changes in engine speed or target pressure, which are the related factors for both the simulated scenario and the measurements. As is shown, a temperature model is not reliable for estimating the fuel temperature for our investigations, since it has a large variation among the scenarios. According to the model, it is possible to have up to 20% error. Because of this high error-rate it is not possible to disregard the error. Adding a temperature sensor could be a solution for this issue. However, this would contribute to the disadvantages of having more hardware, complexity and more wiring. To be able to estimate the amount of the injected fuel, it is necessary to have a sensor or a significantly better calibration of the temperature estimation model used today.

5.2 Results of Delta-Sigma ADC Implementation

In this section, results of the evaluation test on the test rig is presented. As is mentioned in section 3.1.1, there are several scenarios with different conditions. Table 5.2 shows the cases that have been tested in the test rig with the evaluation board. Since these cases are only measured to clarify the delta-sigma ADC implementation the engine speed was kept as a constant at 1200 rpm. The aim of having different cases is to see if the data from delta-sigma conversion is reliable for the ECU.

Table 5.2: The table represents a final measurement in the injection rig together with the real-time implementation. The six cases presented were selected as a proof of concept that the real-time implementation works. Since the common-rail pressure in independent of engine speed only the target pressure and the quantity of the main injection (injected fuel amount) were varied. These cases were also made having a 5 mg/stroke pilot injection.

Case	Target Pressure bar	Main Injection mg/stroke
1	700	360
2	2400	360
3	2400	200
4	2400	20
5	600	20
6	600	100

In each case, first presented figure shows the sampled result of the interrupt, the second one represents the window with maximum and minimum values of each injection showed with data cursors for each interrupt result and the last figure shows the results from the evaluation board.

In case 1 presented in table 5.2, as can be seen in figure 5.9, the interrupt is long enough to store significant amount of data for the pressure drop detection in a digital bit amplitude representation. Figure 5.9 also shows that it would be possible to have a smaller amount of samples for the interrupt since only the pressure decay that is of interest. However, the timing of the sampling is crucial and having more data stored will provide us a certainty that the injection will not be excluded from the stored result.

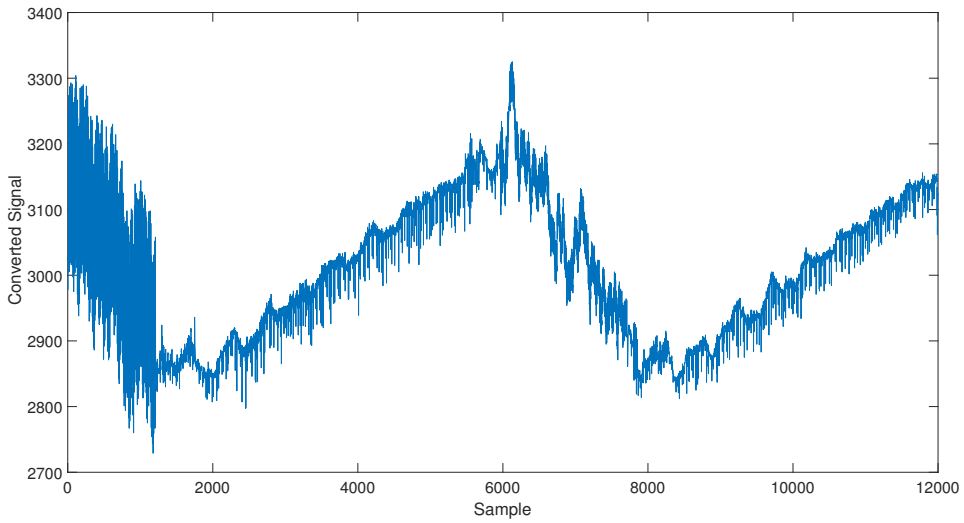

Figure 5.9: The graph above shows a representation for the result register for case 1 from table 5.2 where 12000 samples are stored in the interrupt. Having a result register of 12000 samples will provide the certainty to cover at least one injection, and as can be seen in this case two injections are covered in the register.

Since it is only the pressure drop that is of interest it is not necessary to process the entire result but instead just process a window of the result. In the implementation the window has been chosen to 5000 samples as shown in figure 5.10. It can also be seen that the pressure drop can be estimated to be between 1.51 and 1.247 Volts with the pressure drop ΔP around 0.263 Volts.

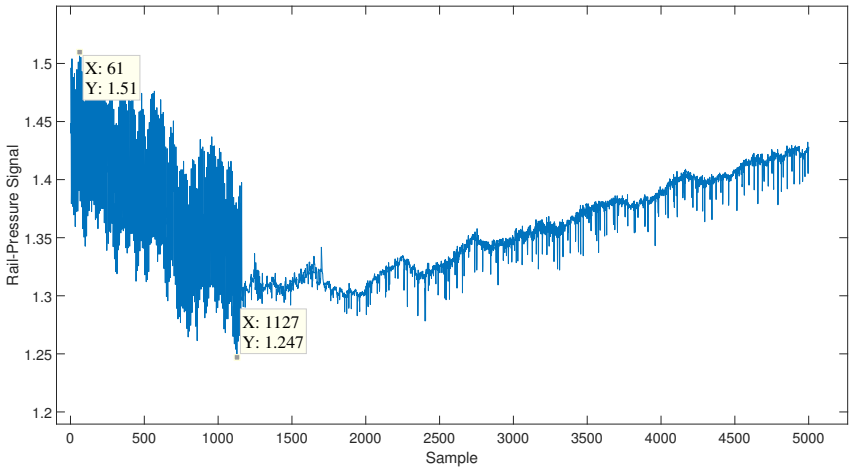

Figure 5.10: The graph above shows the window of 5000 samples used to detect the pressure drop showed in figure 5.9. The DSP function of the real-time implementation detects the max and min value as also presented above as 1.51 and 1.247 Volts.

As mentioned before, 12000 samples are believed to cover at least one injection. As shown in figure 5.11, this also applies for the second case in table 5.2. It can be seen that this case has a higher target pressure since the digital amplitude is higher than for the first case.

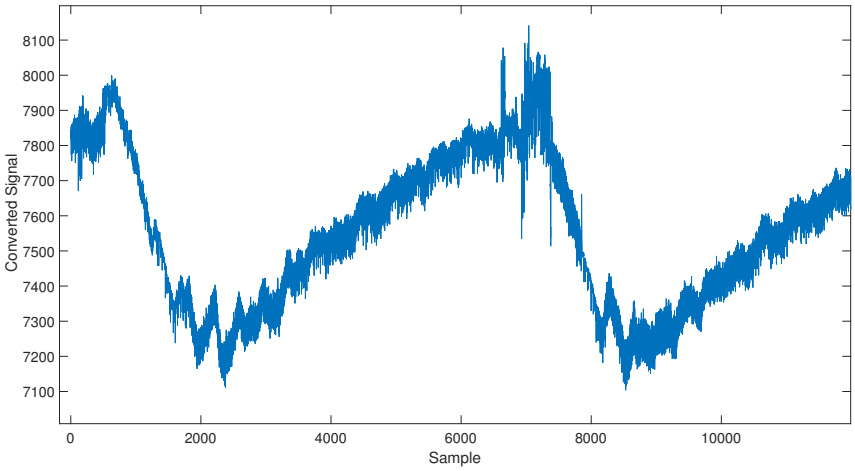

Figure 5.11: The graph above shows a representation for the result register for case 2 from table 5.2 where 12000 samples are stored in the interrupt. As shown in Figure 5.9 also in this case two injections are covered in the register.

Figure 5.12 shows the window of 5000 samples to only contain one injection. As it is shown the max- and min values show 3.655 and 3.274 both in figure 5.12.

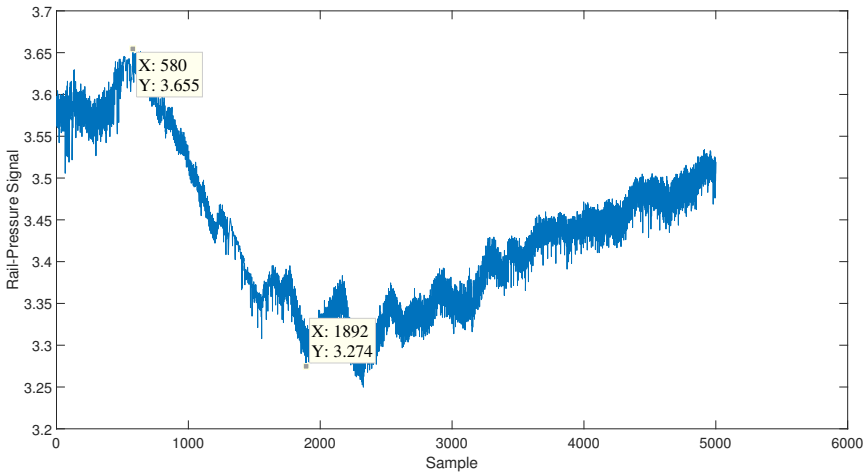

Figure 5.12: The graph above shows the window of 5000 samples used to detect the pressure drop showed in figure 5.11. The DSP function detection of the max and min value as also presented above as 3.655 and 3.274 Volts.

The pressure drop is also detected and calculated to be around 0.406 Volts. This result shows that even the higher target pressure within the same amount gives a larger pressure drop. This shows that the implementation does not seem to be affected result-wise by the rail-pressure change from 700 to 2400 bar. In case 3 from table 5.2, the results are still consistent with the two previous cases. Figure 5.13 show the complete stored results from the interrupt. Moreover, in this case the amount of samples stored are enough to detect at least one injection. It can be seen that the target pressure is still at the same amplitude as for case 2 since the digital amplitude still varies around 7000 to 8000.

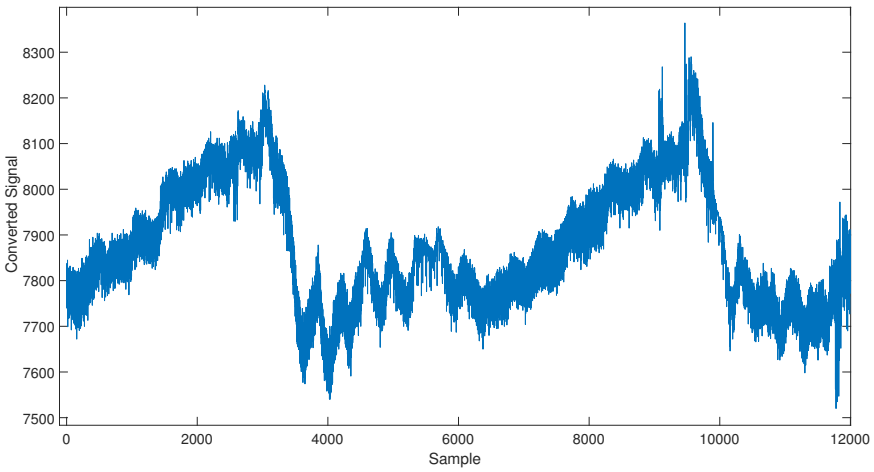

Figure 5.13: The graph above shown in the same way as figure 5.9 and figure 5.11 the whole result register with 12000 samples in the interrupt but for case 3 from table 5.2.

In this case the injected fuel has been lowered to a quantity of 200 mg/stroke instead of 360 mg/stroke as has been for the previous cases. It can be seen in the window of 5000 samples in figure 5.14 that the max- and min values are in this case 3.76 and 3.461 Volts, which both are higher than case 2 that can be due to pressure oscillations or other factors of the common rail. This result shows that the pressure decay is smaller than for a higher amount of injection as for case 2.

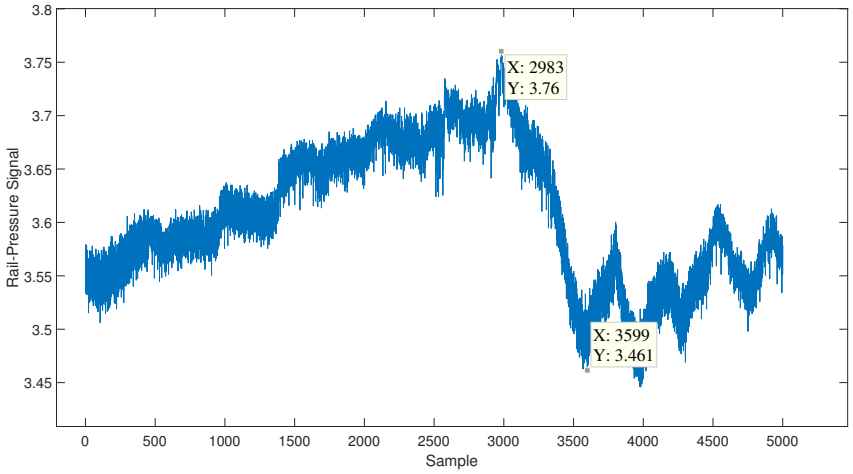

Figure 5.14: The window of 5000 samples shows also in the third case one injection with the max and min value at 3.76 and 3.461 Volts.

Case 4 provides information of how small amounts of injection can be detected. The quantity in case 4 is as presented in table 5.2 to only 20 mg/stroke but still at a target pressure of 2400 bar. The outcome of this low fuel injection is that the injection does not provide any larger pressure variation, as can be seen in figure 5.15, and is still within the noise floor.

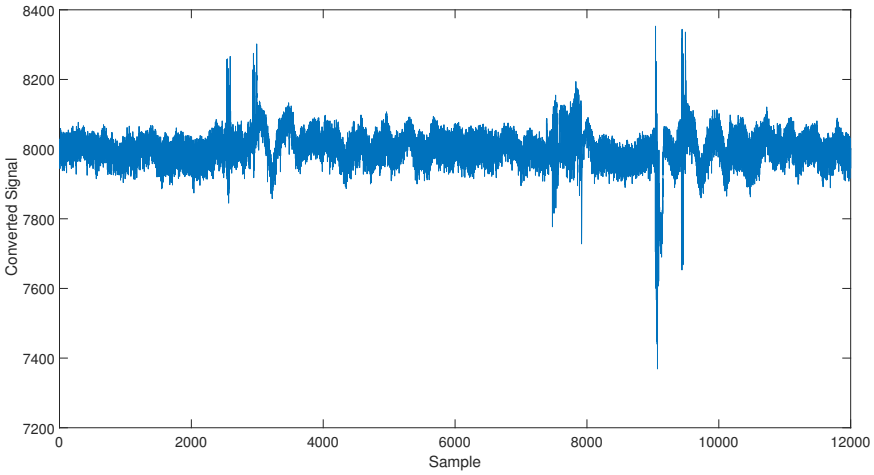

Figure 5.15: The graph above shown in the same way as figure 5.9, figure 5.11 and figure 5.13 the whole result register with 12000 samples in the interrupt but for case 4 from table 5.2. An obvious observation is that this graph looks quite different from to the others. The reason for this is that the target pressure is set high and the injection is quite small. The injection in this particular case is 100 times smaller than in case 3 and does not contribute to as a big a time variance of the rail pressure.

However, as can be seen in figure 5.16, there is something happening in the window. The max- and min values are within the same span as the previous cases as a max value about 3.8 was measured, which is to expected by the other cases. As is shown in figure 5.16, pressure drop is 0.203 Volt.

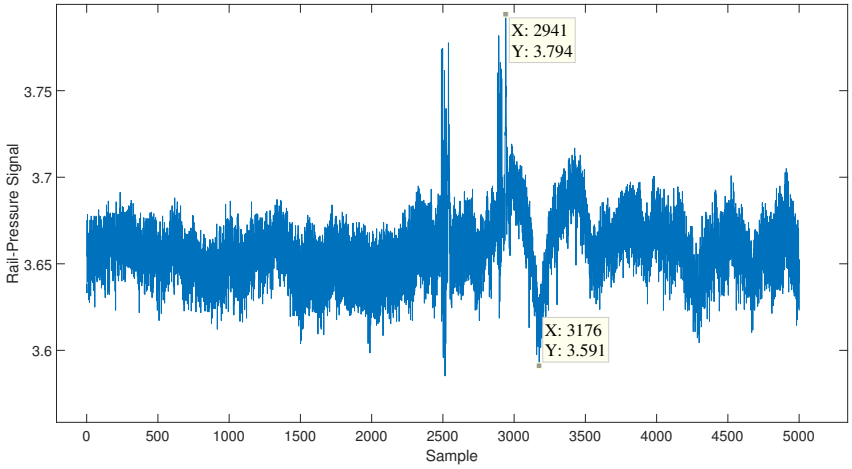

Figure 5.16: The graph above shows the window of 5000 samples to detect the pressure drop in case 4. Even though there is no clear pressure drop in figure 5.15 the max and min value is still detected to 3.794 and 3.591 Volts.

6

Conclusion

The purpose of this project was to investigate how high-speed sampling with a delta-sigma ADC which can provide more accurate data to the ECU. The report has discussed the theory of analog-to-digital conversion together with the principles of what signifies the delta-sigma ADC.

The target of this investigation was to process the common-rail pressure of a diesel-truck engine. The processing of the common rail was used for estimation of injected fuel amount. Since the common rail is a part of the injection system, this report has described the basic concept of the injection system, characteristics of the engine and how the dependencies for fuel estimation are estimated. The work to gather data has been stated as very specific scenarios for different data gathering occasions. This shows the difficulty in having a static measurement setup due to temperature variation and the continuous variations of a running engine.

Another big part of this report has discussed the measurement data and how it has been gathered in a simplified engine environment in which a verification study was also made. This simplified environment has been described as an environment which provides additional information that would otherwise not be possible to obtain. Additional information about the specifics of this environment is limited for this project.

The project has shown that the delta-sigma ADC can convert the rail-pressure signal with high accuracy and it is fast enough to be able to detect the pressure drop in injection. The small pressure variations can be detected by delta-sigma ADC together with Infineon Tricore microprocessor. The reason is that Infineon is fast enough to convert the injection signal to the digital domain and delta-sigma is accurate enough to detect the pressure gap between each injection. Having the pressure differences during an injection allows the ECU to estimate the fuel consumption.

As we expected in pre-study phase, the result is reliable in real-time implementation, since MATLAB implementation has been proved that small amount of injection can be detected accurately. Another result of the project is that noise can be canceled out in the interest frequency of interest due to the noise shaping features. This feature has been demonstrated in both MATLAB and real-time implementation.

However, estimating the exact amount of the fuel injected requires the temperature of the fuel. Since no temperature sensor is installed on the real engine, one has to resort to estimating the fuel temperature, which leads to an enormous error.

One of the most important achievement of the project is that a temperature sensor is required in the engine to be able to estimate the exact amount of the fuel in each injection. This lack of hardware can lead to the error in different scenarios due to the temperature model which is currently used and it is not very accurate. This error cannot be calibrated out since it has a non-linear behavior. The solution to this error can be a temperature sensor to get an exact value of the temperature.

References

[1] B. Baker. *(2011). How delta-sigma ADCs work. (Part 1).* [Online]. Available: http://www.ti.com/lit/an/slyt423a/slyt423a.pdf

[2] Infineon. *(2015-07). Delta Sigma Demodulator.* [Online]. Available: http://www.infineon.com/dgdl/Infineon-DSD-XMC4000-AP32302-AN-v01_00-EN.pdf?fileId=5546d4624e765da5014ed901e8851b1f

[3] H. Jääskeläinen and M. K. Khair. *(2013-11). Combustion in Diesel Engines* [Online]. Available: https://www.dieselnet.com/tech/diesel_combustion.php

[4] H. Jääskeläinen. *(2013-11). Early History of the Diesel Engine.* [Online]. Available: https://www.dieselnet.com/tech/diesel_history.php

[5] W. Kester. *Mixed-signal and DSP Design Techniques.*, Lecture notes, Amesterdam: Newnes,Boston: Elsevier Inc. 2005

[6] T. Schreier and G. Temes *Understanding Delta-Sigma Data Converters,(2005)*, Wiley-IEEE Press

[7] Volvo history. [Online]. Available: http://www.volvotrucks.com/trucks/global/en-gb/aboutus/history/1940s/Pages/LV15_and_LV24.aspx

[8] *(European Standard)* [Online]. Available: https://www.dieselnet.com/standards/eu/hd.php

[9] Cherry and A. James *Continuous-time delta-sigma modulators for high-speed A/D/ conversion : theory, practice, and fundamental performance limits. (2000)*

[10] H. Jääskeläinen and M. K. Khair. *(2015.05). Common Rail Fuel Injection*[Online]. Available: https://www.dieselnet.com/tech/diesel_fi_common-rail.php

[11] *(206-07). Harman Grewal.* [Online]. Available: http://www.ti.com/lit/an/slaa323/slaa323.pdf

[12] M. K. Khair and H. Jääskeläinen. *(2015-02). Emission Formation in Diesel Engines* [Online]. Available: https://www.dieselnet.com/tech/diesel_emiform.php

[13] ISO-Standard 4113. *Thermophysical properties of Normafluids,(2015-02)*, Retrieved from ISO-Standard archives

[14] Chorążewski et al. (2013). Thermophysical properties of normafluid (ISO 4113) over wide pressure and temperature ranges. Fuel, 105, 440-450.

[15] F. Maloberti. (2007). SpringerLink Data converters. Dordrecht, Netherlands: Springer. doi:10.1007/978-0-387-32486-9

[16] Clever. Insermann:*Model-based fault detection and diagnosis for common-rail inection systems*, (2009-11-01) Technische Universität Darmstadt, Germany

[17] *AURIX TC29x starter kit.* [Online]. Available: https://www.ehitex.de/en/starter-kits/for-aurix/2518/aurix-starter-kit-tc297?c=157

[18] *Yokogawa DLM4000.* [Online]. Available: http://tmi.yokogawa.com/es/products/oscilloscopes/digital-and-mixed-signal-oscilloscopes/dlm4000-mso-series/

[19] *Tricore tool chain based on the Eclipse*[Online]. Available: http://www.infineon.com/cms/en/product/microcontroller/32-bit-tricore-tm-microcontroller/tricore-tm-development-tools-software-and-kits/free-tricore-entry-tool-chain/channel.html?channel=db3a304344134c7a014420d628fa76ec

A

Appendix

Figure A.1: Photograph of the rig which was used to collect measurement data.

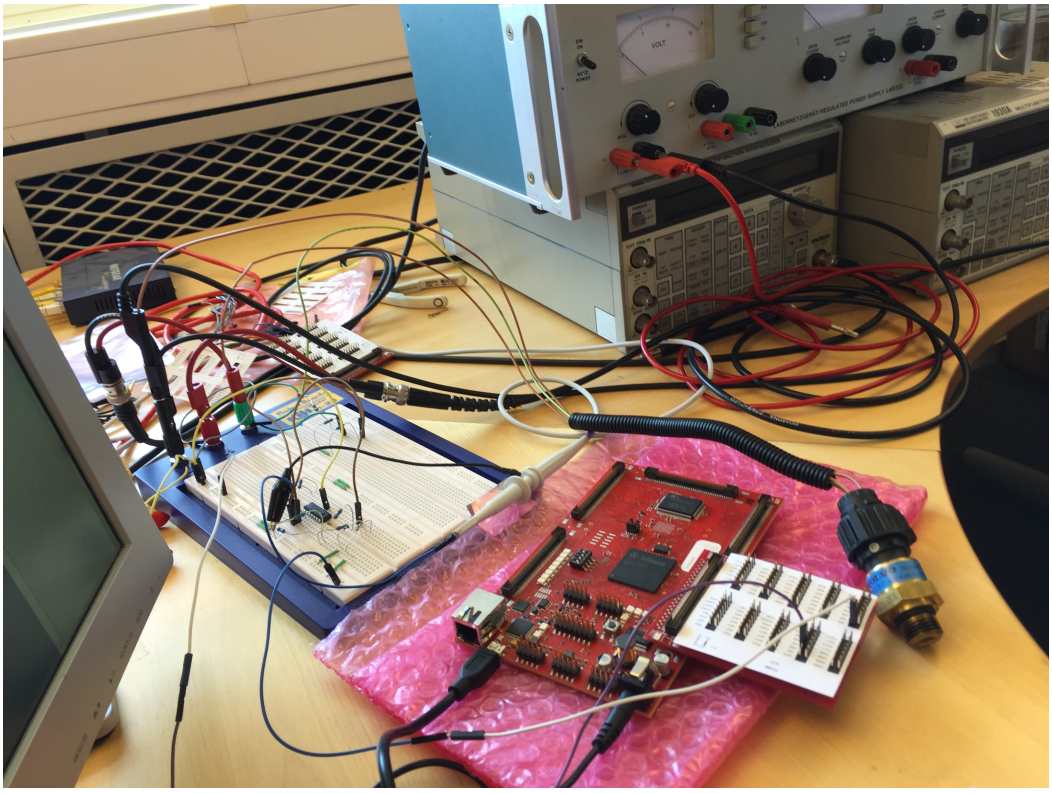

Figure A.2: Photograph of the realtime implementation of the delta-sigma ADC. The photograph shows the project board, function generators, voltage supplier and the Infineon evaluation board